



**HAL**  
open science

# **Burkholderia insecticola triggers midgut closure in the bean bug *Riptortus pedestris* to prevent secondary bacterial infections of midgut crypts**

Yoshitomo Kikuchi, Tsubasa Ohbayashi, Seonghan Jang, Peter Mergaert

► **To cite this version:**

Yoshitomo Kikuchi, Tsubasa Ohbayashi, Seonghan Jang, Peter Mergaert. *Burkholderia insecticola* triggers midgut closure in the bean bug *Riptortus pedestris* to prevent secondary bacterial infections of midgut crypts. *The International Society of Microbiological Ecology Journal*, 2020, 10.1038/s41396-020-0633-3 . hal-03375705

**HAL Id: hal-03375705**

**<https://hal.science/hal-03375705>**

Submitted on 13 Oct 2021

**HAL** is a multi-disciplinary open access archive for the deposit and dissemination of scientific research documents, whether they are published or not. The documents may come from teaching and research institutions in France or abroad, or from public or private research centers.

L'archive ouverte pluridisciplinaire **HAL**, est destinée au dépôt et à la diffusion de documents scientifiques de niveau recherche, publiés ou non, émanant des établissements d'enseignement et de recherche français ou étrangers, des laboratoires publics ou privés.

1 ***Burkholderia insecticola* triggers midgut closure in the bean bug *Riptortus pedestris* to**  
2 **prevent secondary bacterial infections of midgut crypts**

3

4 Yoshitomo Kikuchi<sup>1,2,3</sup>, Tsubasa Ohbayashi<sup>4,5</sup>, Seonghan Jang<sup>3</sup> and Peter Mergaert<sup>4</sup>

5

6 <sup>1</sup>Bioproduction Research Institute, National Institute of Advanced Industrial Science and  
7 Technology (AIST), Hokkaido Center, 062-8517 Sapporo, Japan

8 <sup>2</sup>Computational Bio Big Data Open Innovation Laboratory (CBBD-OIL), AIST, 062-8517  
9 Sapporo, Japan

10 <sup>3</sup>Graduate School of Agriculture, Hokkaido University, 060-8589 Sapporo, Japan

11 <sup>4</sup>Université Paris-Saclay, CEA, CNRS, Institute for Integrative Biology of the Cell (I2BC),  
12 91198 Gif-sur-Yvette, France

13 <sup>5</sup>Institute for Agro-Environmental Sciences, National Agriculture and Food Research  
14 Organization (NARO), 305-8604 Tsukuba, Japan

15

16 Correspondence: Yoshitomo Kikuchi (y-kikuchi@aist.go.jp)

17

18

19 **Abstract**

20 In addition to abiotic triggers, biotic factors such as microbial symbionts can alter  
21 development of multicellular organisms. Symbiont-mediated morphogenesis is  
22 well-investigated in plants and marine invertebrates but rarely in insects despite the enormous  
23 diversity of insect-microbe symbioses. The bean bug *Riptortus pedestris* is associated with  
24 *Burkholderia insecticola* which are acquired from the environmental soil and housed in  
25 midgut crypts. To sort symbionts from soil microbiota, the bean bug develops a specific organ  
26 called the “constricted region” (CR), a narrow and symbiont-selective channel, located in the  
27 midgut immediately upstream of the crypt-bearing region. In this study, inoculation of  
28 fluorescent protein-labelled symbionts followed by spatiotemporal microscopic observations  
29 revealed that after the initial passage of symbionts through the CR, it closes within 12 to 18  
30 hours, blocking any potential subsequent infection events. The “midgut closure”  
31 developmental response was irreversible, even after symbiont removal from the crypts by  
32 antibiotics. It never occurred in aposymbiotic insects, nor in insects infected with  
33 non-symbiotic bacteria or *B. insecticola* mutants unable to cross the CR. However, species of  
34 the genus *Burkholderia* and its outgroup *Pandoraea* that can pass the CR and partially  
35 colonize the midgut crypts induce the morphological alteration, suggesting that the molecular  
36 trigger signaling the midgut closure is conserved in this bacterial lineage. We propose that this  
37 drastic and quick alteration of the midgut morphology in response to symbiont infection is a  
38 mechanism for stabilizing the insect-microbe gut symbiosis and contributes to host-symbiont  
39 specificity in a symbiosis without vertical transmission.

40

41 **Introduction**

42 Phenotypic alteration in response to environmental factors is omnipresent in nature, and is  
43 thought to be a driving force for generation of evolutionary novelty (1). In plants and  
44 animals that are intimately associated with microbes, the symbiont acquisition is integrated  
45 in the hosts' development and sometimes triggers dramatic developmental responses.  
46 Well-known examples are found in the root nodule formation of the legume-*Rhizobium*  
47 symbiosis and the light organ morphogenesis of the squid-*Vibrio* symbiosis (2, 3). Besides  
48 such drastic morphological changes in specific associations, recent studies on mammals and  
49 *Drosophila* gut microbiota have revealed that gut bacteria also play a significant role in  
50 proliferation and differentiation of gut epithelial cells and in metabolic and immunity  
51 homeostasis (4, 5). Similarly, in the plant kingdom, rhizosphere microbiota modify the root  
52 and shoot architecture by modulating the phytohormone balance in the plant (6). Even  
53 non-symbiotic, environmental bacteria can have profound morphological effects on  
54 eukaryotes by the production of small molecules that act as essential developmental cues.  
55 The settlement and subsequent metamorphosis of free-swimming larvae of the marine  
56 tubeworm *Hydroides elegans* are triggered by biofilms of the bacterium *Pseudoalteromonas*  
57 *luteoviolacea*. These biofilms deliver a metamorphosis-triggering effector protein into the  
58 larvae via a contractile injection system (7-9). Another striking example is the triggering of  
59 multicellularity from a single founder cell in the choanoflagellate *Salpingoaecca rosetta* by a  
60 sulfonolipid, derived from specific prey bacteria of the Bacteroidetes (10).

61         The class Insecta consists of over one million described species and is the most  
62 diverse animal group in the terrestrial ecosystem. Many insects harbor symbiotic bacteria in  
63 specialized cells called bacteriocytes or in gut crypts (11, 12). In these symbiotic organs,

64 bacterial symbionts play metabolic roles for the hosts, such as provision of essential  
65 nutrients and/or digestion of indigestible food materials (13-15). Recent studies have  
66 revealed that, in addition, symbionts alter diverse aspects of host phenotypes, including heat  
67 tolerance, pathogen resistance, behavior, sex, cuticle hardening, body color, and tolerance to  
68 phytotoxins and insecticides (16-23). Despite the accumulated knowledge about the diverse  
69 symbiosis-mediated phenotypes, symbiont-induced morphogenesis of the symbiotic organ  
70 has been poorly described in insects.

71         The bean bug *Riptortus pedestris* develops a number of crypts in a posterior region  
72 of the midgut, the lumen of which is densely colonized by the betaproteobacterial symbiont,  
73 *Burkholderia insecticola* (24-27). Infection with *B. insecticola* improves growth and  
74 fecundity of the bean bug (28) probably because the symbiont recycles host metabolic  
75 wastes in the midgut crypts (29). Unlike the typical insect-microbe symbioses in which  
76 symbionts are vertically transmitted from mother to offspring, the bean bug acquires *B.*  
77 *insecticola* from environmental soil every generation (30). From hatching to adulthood, the  
78 bean bug development passes over five instar stages and the symbiont is acquired  
79 preferentially at the 2<sup>nd</sup> instar but also 3<sup>th</sup> instar nymphs are compatible for infection (31).

80         Since diverse microorganisms abound in the environment, particularly in soils (32),  
81 hosts need to sort their specific partner from this microbial community. Furthermore, after  
82 symbiont colonization, they have to protect the symbiotic organ against invasion by  
83 superinfection to stabilize the mutualistic association. To sort the symbiont, the bean bug  
84 develops a specific organ called the “constricted region” (CR), a narrow passage filled with  
85 a mucus-like matrix, located in the midgut immediately upstream of the crypt-bearing  
86 region (33). The CR sorts out contaminating microorganisms while *B. insecticola* can

87 penetrate into the symbiotic region using an unusual, corkscrew-like flagellar motility  
88 (33-35). However, the sorting mechanism is not perfectly tight and some allied  
89 non-symbiont *Burkholderia* species as well as species of its outgroup *Pandoraea* can  
90 nevertheless penetrate the CR (36). Interestingly, the non-native *Burkholderia* and  
91 *Pandoraea* species do not fully occupy the lumen of the midgut crypts and co-inoculation  
92 analyses revealed that *B. insecticola* always outcompetes these non-native bacteria inside  
93 the crypts, suggesting that the crypt's luminal environment favors only the native symbiont  
94 (36). Although the molecular basis remains unclear, the competition-based winnowing is  
95 therefore, thought of as a second-line mechanism ensuring the host-symbiont specificity. In  
96 addition to these partner choice mechanisms, here we discovered a third mechanism  
97 underpinning the specific gut symbiosis which we call "midgut closure", wherein the CR is  
98 closed immediately after colonization of the crypt-bearing midgut region by the symbiont,  
99 preventing subsequent infections.

100

## 101 **Materials and methods**

### 102 **Insects and bacterial strains**

103 The strain of *R. pedestris* used in this study was originally collected from a soybean  
104 (*Glycine max*) field in Tsukuba, Ibaraki, Japan, and maintained in the laboratory over ten  
105 years. The insects were reared in petri dishes (90 mm in diameter and 20 mm high) at 25°C  
106 under a long-day regimen (16 h light, 8 h dark) and fed with soybean seeds and distilled  
107 water containing 0.05% ascorbic acid (DWA). For inoculation tests of  
108 fluorescent-protein-labelled *B. insecticola*, a green fluorescent protein (GFP)-labelled strain,  
109 RPE225 (28), and a red fluorescent protein (RFP)-labelled strain, KT39 (36), were used. *B.*

110 *insecticola* derivatives, including gene-deletion mutants, and non-symbiotic bacteria used in  
111 this study are listed in [Supplementary Table S1](#). They were labeled with GFP using the Tn7  
112 minitransposon system, as previously described (28, 37).

113

#### 114 **Oral inoculation of cultured symbiont cells**

115 The symbiont strains were grown to early log phase in YG medium (containing 30 µg/ml  
116 kanamycin for GFP-labelled RPE225 and RFP-labelled KT39) on a gyratory shaker (150  
117 rpm) at 30°C. Bacteria were harvested by centrifugation, re-suspended in DWA, and  
118 adjusted to 10<sup>4</sup> cells/µl in DWA. Three types of inoculations were performed: (i) oral  
119 inoculation of the GFP strain at the 2<sup>nd</sup> instar, (ii) oral inoculation of the GFP strain at the 3<sup>rd</sup>  
120 instar, and (iii) oral inoculation of the RFP strain at the 2<sup>nd</sup> and then the GFP strain  
121 inoculated after a defined interval.

122 (i) Oral inoculation of the GFP strain at 2<sup>nd</sup> instar. Immediately after 1<sup>st</sup> instar  
123 nymphs molted to the 2<sup>nd</sup> instar, DWA was removed from the rearing containers so that the  
124 nymphs were kept without drinking water overnight. Then 1 µl DWA containing 10<sup>4</sup> cells/µl  
125 of the GFP-labelled RPE225 was supplied to the rearing containers, which the 2<sup>nd</sup> instar  
126 nymphs immediately exploited, leading to the acquisition of *Burkholderia* symbionts. After  
127 drinking, insects were supplied with DWA and the nymphs were further reared in the  
128 absence of bacteria for variable times before dissection to analyze their infection status as  
129 described below.

130 (ii) Oral inoculation of the GFP strain at 3<sup>rd</sup> instar. Nymphs were kept with soybean  
131 seeds and symbiont-free DWA until the 2<sup>nd</sup> instar. Immediately after 2<sup>nd</sup> instar nymphs  
132 molted to the 3<sup>rd</sup> instar, the DWA was removed from the rearing containers so that the

133 nymphs were kept without drinking water overnight. Then 1  $\mu$ l DWA containing  $10^4$  cells/ $\mu$ l  
134 of the GFP-labelled RPE225 was supplied to the rearing containers, which the 3<sup>rd</sup> instar  
135 nymphs immediately exploited, leading to the acquisition of *Burkholderia* symbionts. After  
136 drinking, insects were supplied with DWA and the nymphs were further reared in the  
137 absence of bacteria for variable times before dissection to analyze their infection status as  
138 described below.

139 (iii) Oral inoculation of the RFP strain, and re-inoculation of the GFP strain after  
140 an interval. After 2<sup>nd</sup> instar molting, DWA was removed so that nymphs became thirsty, as  
141 described above. Then 1  $\mu$ l DWA containing  $10^4$  cells/ $\mu$ l of the RFP-labelled strain, KT39,  
142 was orally inoculated to the 2<sup>nd</sup> instar nymphs. After drinking the bacteria-containing DWA,  
143 insects were kept with soybean seeds for 6 h, 12 h, 15 h, 18 h, or 3 days. After the interval,  
144 1  $\mu$ l DWA containing  $10^4$  cells/ $\mu$ l of the GFP-labelled RPE225 was supplied to the rearing  
145 containers. As for the first infection, insects were deprived of water before the second  
146 infection. These nymphs were further reared for two days with symbiont-free DWA, and  
147 then dissected to check their infection status of the RFP and GFP strains. In the  
148 3-day-interval group, insects became 3<sup>rd</sup> instar during the interval, and the molted nymphs  
149 were subjected to the re-inoculation test.

150

### 151 **Experimental removal of crypt-colonizing symbionts by antibiotic treatment**

152 To investigate the plasticity of the midgut closure, experimental removal of crypt-colonized  
153 *B. insecticola* by antibiotic treatment followed by re-inoculation of the symbiont was  
154 performed. For this experiment, a chloramphenicol (Cm)-susceptible GFP-labelled strain,  
155 KT33, and a Cm-resistant RFP-labelled strain, RPE744, were used ([Supplementary Table](#)

156 S1). The GFP-labelled Cm- susceptible KT33 was constructed by the Tn7 minitransposon  
157 system (37), while the RFP-labelled Cm-resistant RPE744 strain carried the stable plasmid  
158 pIN29 (38). Immediately after 1<sup>st</sup> instar nymphs molted to the 2<sup>nd</sup> instar, DWA was removed  
159 from the rearing containers and the nymphs were kept without drinking water overnight.  
160 Then DWA containing 10<sup>4</sup> cells/μl of the GFP-labelled Cm- susceptible strain KT33 was  
161 supplied to the rearing containers for 24 h. After 24 h, the symbiont-containing DWA was  
162 replaced by DWA containing 100 μg/ml chloramphenicol to remove the symbiont. Insects  
163 were treated with the antibiotic during the 2<sup>nd</sup> instar stage, and after molting to the 3<sup>rd</sup> instar,  
164 the Cm-resistant RFP-labelled strain RPE744 was inoculated as described above. These  
165 nymphs were further reared for two days with symbiont-free DWA, and then dissected to  
166 check their infection status with the GFP or RFP strains. To verify the first treatments in the  
167 2<sup>nd</sup> instar stage, half of the treated insects (10 insects/20 in total) were sacrificed in the  
168 second instar, dissected and their infection status was verified. In addition, two types of  
169 control experiments were performed: first, insects were treated with chloramphenicol but  
170 without inoculation of the GFP strain in the 2<sup>nd</sup> instar stage, and then the RFP-labelled  
171 RPE744 strain was inoculated after molting to the 3<sup>rd</sup> instar; second, insects were inoculated  
172 with the GFP-labelled symbiont at the 2<sup>nd</sup> instar stage without chloramphenicol treatment,  
173 and the insects were inoculated with the RFP-labelled RPE744 at the 3<sup>rd</sup> instar stage.

174

175 Methods for “microscopic observations of dissected symbiotic organs”, “oral inoculation of  
176 colonization-deficient mutants and non-symbiotic bacteria” and “bottleneck estimation” are  
177 described in the [Supplementary Information](#).

178

179 **Results**

180 **Closure of the constricted region during symbiont colonization**

181 The midgut of *R. pedestris* consists of four distinct sections called M1, M2, M3 and M4  
182 (Supplementary Fig. S1). The symbiotic *Burkholderia* specifically colonizes the  
183 crypt-bearing M4 section. In front of M4, a distinct, bulbous part called the M4 bulb (M4B)  
184 is developed, wherein symbionts flow from the M4 section and are digested (29, 39). The  
185 M3 and M4B are connected by the CR. Our previous study using a GFP-labelled  
186 *Burkholderia* symbiont revealed that in the 2<sup>nd</sup> instar, colonization of the symbiotic  
187 M4B-M4 region of the midgut starts around 6 hours post inoculation (hpi) (28). Around 24  
188 hpi, the symbiont cells appear in the main tract of the M4 region and start the colonization  
189 of the crypts. At 48 hpi most of the crypts are colonized and around 72 hpi, crypts are  
190 entirely filled by the symbiont cells. This colonization pattern is then stably maintained  
191 during the subsequent nymphal stages.

192 In order to further detail the dynamics of the infection process, we performed  
193 time course observations focusing on the CR and M4B regions of the midgut. As described  
194 before, the infection from M3 to M4B through the CR started around 6 hpi and a continuous  
195 migration of GFP-labeled bacteria was observed (Fig. 1a and b; Supplementary Fig. S2).  
196 However, around 15 hpi the connection was abruptly interrupted, despite the continuous  
197 presence of a dense population of symbiont cells in the M3 (Fig. 1c and d; Supplementary  
198 Fig. S2). Subsequently, the M4B was further closed from the side of the CR, and the closure  
199 was accomplished around 24 hpi (Fig. 1e-h; Supplementary Fig. S2). Laser Scanning  
200 Microscopy (LSM) observations revealed that after symbiont colonization, at 24 hpi, the  
201 epithelial cells of M4B are bulged at the luminal side and are arranged like interlocking

202 teeth, closed like a zipper (Fig. 2a and b).

203           In the M4 crypts, the *Burkholderia* symbionts started colonization from 12 hpi,  
204 and then proliferated in them until they fully occupied the crypts by 48 hpi (Supplementary  
205 Fig. S3). Notably, in parallel with the filling of crypts, symbiont cells started to flow  
206 backwards from M4 into M4B around 36-42 hpi (Fig. 1i-l; Supplementary Fig. S2). M4B  
207 was entirely filled by symbiont cells and became bulbous and matured around 48 hpi  
208 (Fig. 1m-r; Supplementary Fig. S2). However, no overflow was observed from M4B to M3,  
209 which at this stage became free of symbionts. LSM observations of tissues stained with  
210 phalloidin showed that the CR is kept tightly closed (Fig. 2c and d). The closure and  
211 re-opening of M4B were not observed in aposymbiotic insects (Fig. 3a-g). Serial  
212 measurements of the CR and M4B (Supplementary Fig. S4) confirmed the marked  
213 morphological changes of the CR (Fig. 1s) and M4B (Fig. 1t) after symbiont infection.

214

### 215 **Symbiont infection of 3<sup>rd</sup> instar nymphs triggers midgut closure**

216 Our previous study reported that the symbiont acquisition occurs mainly at the 2<sup>nd</sup> instar but  
217 3<sup>rd</sup> instar nymphs are still competent to acquire the symbiont (31). To demonstrate the  
218 symbiont-dependency of the gut morphological alteration, we kept insects aposymbiotic  
219 during the 2<sup>nd</sup> instar, and then inoculated symbiont cells after molting and entry into the 3<sup>rd</sup>  
220 instar (Fig. 3a). While the closure and re-opening of M4B were not observed in the  
221 aposymbiotic 2<sup>nd</sup> instar stage (Fig. 3b-g), the insects that ingested the symbionts at the 3<sup>rd</sup>  
222 instar stage showed the closure and re-opening of M4B after symbiont infection in a similar  
223 way as during 2<sup>nd</sup> instar infection and colonization (Fig. 3h-m). However, the response time  
224 in the 3<sup>rd</sup> instar stage was delayed compared with the 2<sup>nd</sup> instar stage (Fig. 1). These results

225 clearly demonstrated that the drastic morphological alteration of the midgut is triggered by  
226 the symbiont.

227

### 228 **Midgut closure blocks super-infection of the M4 crypts**

229 To confirm the physical closure of the CR after the symbiont colonization, a re-inoculation  
230 test of the symbiont was performed, in which a GFP-labelled symbiont is inoculated to  
231 nymphs that already acquired an RFP-labelled symbiont ([Supplementary Fig. S5a](#)). Insects  
232 accepted GFP-labelled symbionts when the symbionts were re-inoculated after short, 6-12 h,  
233 intervals ([Supplementary Fig. S5b, Fig. S6](#)). However, insects only rarely acquired the  
234 GFP-labelled symbionts when the bacteria were re-inoculated after a 15 h interval  
235 ([Supplementary Fig. S5b, Fig. S6](#)), which strikingly corresponded to the start of the midgut  
236 closure observed by microscopy ([Fig. 1](#)), and it never happened when the interval was  
237 longer ([Supplementary Fig. S5b, Fig. S6](#)).

238         Accordingly, when the GFP-labelled symbiont was inoculated to 3<sup>rd</sup> instar  
239 nymphs that already acquired the RFP-labelled symbiont during the 2<sup>nd</sup> instar stage ([Fig. 4a](#)),  
240 insects never acquired the GFP-labelled symbiont ([Supplementary Fig. S5b, Fig. S6](#)). LSM  
241 observations revealed that, after colonization of the symbiotic region by an RFP-labelled  
242 symbiont, no GFP-labelled symbionts were able to enter the CR, although the GFP-labelled  
243 symbiont cells were readily detected in the M3 region ([Fig. 4b and c](#)). These results  
244 confirmed that the morphological closure of the CR after symbiont colonization in M4  
245 crypts and maturation of M4B, effectively prevents subsequent entry of bacteria in the  
246 symbiotic organ.

247

248 **The midgut closure is correlated with a bottleneck of symbiont infection**

249 The rapid closing of the CR, together with its narrow diameter of a few micrometers (33)  
250 could constrict the number of bacteria that can transit from M3 into M4 and thus cause a  
251 bottleneck of symbiont infection. Then, how many symbiont cells can enter the symbiotic  
252 region before the closing? To determine the bottleneck size, GFP-labelled symbiont cells  
253 were co-inoculated with non-labelled wild type symbiont cells in different ratios ranging  
254 from one in ten to one in  $2 \times 10^5$ . The total inoculum per insect was adjusted to  $10^5$  CFU  
255 throughout the experiments. The rationale of the experiment was that if the dilution factor of  
256 the GFP-labelled strain is below the bottleneck, the marked strain should readily colonize  
257 the crypts while it should not when the dilution factor is higher than the bottleneck. If the  
258 dilution factor is around the bottleneck size, some insects should be infected and others not  
259 with the GFP-marked strain. Based on the detection rate of GFP-labelled symbiont cells, we  
260 concluded that the bottleneck of symbiont infection is 3,950 cells under the used  
261 experimental conditions ([Supplementary Fig. S7](#)).

262

263 **Midgut closure is permanent**

264 To investigate the plasticity of the midgut closure, an experimental symbiont removal and  
265 re-inoculation test was performed. During the 2<sup>nd</sup> instar stage, a GFP-labelled and  
266 chloramphenicol sensitive symbiont was allowed to establish in the M4 crypts and was  
267 subsequently removed by chloramphenicol treatment. An RFP-labelled and  
268 chloramphenicol resistant symbiont was then re-inoculated at the 3<sup>rd</sup> instar stage ([Fig. 5a](#)).  
269 The chloramphenicol treatment during the 2<sup>nd</sup> instar stage efficiently removed the  
270 GFP-labelled symbiont cells from the crypts and the insects became aposymbiotic

271 (GFP-Cm in Fig. 5b). The removal was complete since the GFP-labelled symbionts did not  
272 reappear after the stop of the chloramphenicol treatment in the 3<sup>rd</sup> instar insects  
273 (GFP-Cm-RFP in Fig. 5c). Despite this complete elimination of the GFP-labelled symbionts  
274 of the first inoculum, no RFP-labelled symbiont was detected in 3<sup>rd</sup> instar nymphs when the  
275 RFP-labelled symbiont was re-inoculated to the cured insects (GFP-Cm-RFP in Fig. 5c). In  
276 control experiments, the re-inoculated RFP-labelled symbiont was accepted when insects  
277 were treated with chloramphenicol without inoculation with the GFP-labelled symbiont  
278 during the 2<sup>nd</sup> instar stage (Cm-RFP in Fig. 5c). On the other hand, the re-inoculated  
279 RFP-labelled symbiont was rejected when a GFP-labelled symbiont was inoculated but not  
280 cured by chloramphenicol during the 2<sup>nd</sup> instar stage (GFP-RFP in Fig. 5c). These results  
281 indicate that there is no phenotypic plasticity in the midgut closure (*i.e.* no re-opening of the  
282 closed region) and that the closure is maintained once it is triggered, even in the absence of  
283 colonizing symbiont cells in the M4 region.

284

### 285 **Triggering of midgut closure by colonization-deficient mutants and non-symbiotic** 286 **bacteria**

287 The rapid midgut closure after infection with the symbiont and its absence in aposymbiotic  
288 insects suggest that the passage of bacteria through the CR and/or the colonization of the  
289 crypts are required to trigger this developmental response. To test this hypothesis directly, a  
290 re-inoculation test of the symbiont was performed, wherein an RFP-labelled *B. insecticola*  
291 was inoculated to nymphs that already acquired a GFP-labelled strain of either  
292 colonization-deficient mutants of *B. insecticola* or non-symbiotic bacteria (Fig. 6a). The  
293 following colonization-defective gene-deletion mutants were used: the flagellar mutant

294 *fliC::Tn5* which can reach M3 but is completely blocked by the CR (33) and the purine  
295 biosynthesis mutant *purL::Tn5* (40), the LPS biosynthesis mutant  $\Delta waaF$  (41) and the PHA  
296 biosynthesis mutant  $\Delta phaB$  (42), which can each reach the crypts but cannot proliferate well  
297 leading to poor crypt colonization. The insects inoculated with the *fliC::Tn5* mutant were  
298 colonized by wild-type *B. insecticola* after re-inoculation indicating no midgut closure by  
299 this mutant (Fig. 6c). On the contrary, the *purL::Tn5*,  $\Delta waaF$ , and  $\Delta phaB$  mutants induced  
300 the midgut closure as evidenced by the complete block of infection by the re-inoculated  
301 wild type (Fig. 6d-f).

302 As non-symbiotic bacteria, the following four species were inoculated:  
303 *Escherichia coli* and *Cupriavidus taiwanensis* which are both blocked at the CR;  
304 *Burkholderia fungorum* and *Pandoraea norimbergensis* which can both pass through the  
305 CR and partially colonize the midgut crypts (36). Insects inoculated with *E. coli* or *C.*  
306 *taiwanensis* did not induce the midgut closure and were colonized by wild-type *B.*  
307 *insecticola* after re-inoculation (Fig. 6g and h). In contrast, *B. fungorum* and *P.*  
308 *norimbergensis* induced the midgut closure and completely blocked the re-inoculated wild  
309 type (Fig. 6i and j). Together, these experiments confirm that the midgut closure is triggered  
310 only when bacteria have entered the symbiotic organ while their presence in the M3 is not  
311 sufficient.

312

### 313 **Discussion**

314 Our previous study reported that the bean bug *R. pedestris* develops in the midgut a  
315 mucus-filled sorting organ, the CR. This unusual organ selects the symbiotic *Burkholderia*  
316 from the enormously diverse soil microorganisms that can penetrate the intestine during

317 feeding and drinking (33). Through the detailed observations of the symbiont infection  
318 process in the 2<sup>nd</sup> instar stage, we revealed here additional important features of this  
319 selection mechanism. Our observations showed that: (i) the CR as well as the M4B are  
320 closed in response to symbiont infection (Fig. 1, Fig. 2; Supplementary Fig. S2); the  
321 morphological alteration of the M4B and the CR did not occur in aposymbiotic nymphs, but  
322 was reproduced in 3<sup>rd</sup> instar nymphs when insects were reared in the absence of bacteria in  
323 the 2<sup>nd</sup> instar and then inoculated after molting (Fig. 3); (ii) after the closure, the symbiont  
324 cells proliferating in the M4 crypts flow back into M4B, which opens again and becomes  
325 bulbous and filled with symbiont cells (Fig. 1; Supplementary Fig. S2); (iii) in spite of the  
326 M4B opening, the CR is kept closed (Fig. 2), blocking any further infection events (Fig. 4);  
327 (iv) once triggered, the CR is kept closed permanently, even when symbionts are removed  
328 from the crypts by antibiotic treatment (Fig. 5); (v) to triggered the closure, the passage of  
329 bacteria - symbionts or other species capable to do so - through the CR and their installation  
330 in the crypts is required (Fig. 6) and (vi) the midgut closure imposes an infection bottleneck  
331 on the symbiont population, limiting the founding population that will populate the  
332 symbiotic organ to a maximum of a few thousand cells (Supplementary Fig. S7). Together,  
333 these results demonstrate that the establishment of bacteria in the midgut crypts provokes a  
334 marked and rapid morphogenic response in the symbiotic organ, which is already largely  
335 formed before the establishment of the symbiosis. To our knowledge, this is a rare example  
336 in the insects of symbiotic microorganisms that trigger a developmental alteration.

337 In contrast to the intracellular symbioses that are typically found in insects, the gut  
338 symbiotic association of *R. pedestris* and related stinkbugs is an open system and the M4  
339 symbiotic organ is in direct contact with the digestive tract, located upstream in the intestine

340 (the M1 to M3 midgut regions). Therefore, the symbiotic organ faces a constant risk of  
341 invasion by other microorganisms, including cheaters and potential pathogens. From this  
342 point of view, the midgut closure found in the bean bug is one of the ultimate mechanisms  
343 to limit contamination of the gut symbiotic organ by unwanted microbes. Indeed, the  
344 re-inoculation test of the *Burkholderia* symbiont clearly demonstrated that the closure  
345 effectively prevents entrance of bacteria once the symbiont is established in the M4B-M4  
346 region (Fig. 4; Supplementary Fig. S5). Moreover, the midgut closure operates within an  
347 intestinal organ that has a very distinctive organization and functioning. The bean bug  
348 externally digests the content of seeds of leguminous plants and sucks up liquid food (43).  
349 By use of food colorings, we showed before that ingested liquid food is completely digested  
350 in M3 and absorbed into the hemolymph (33) and never enters the M4B and M4 region.  
351 Thus the symbiotic organ is isolated from the digestive flow in the intestine and this  
352 disconnection is independent of the symbiosis since it is established already in aposymbiotic  
353 animals (33). Metabolic wastes are removed by the malpighian tubes and excreted via the  
354 hindgut, although transcriptome analyses suggest that some metabolic wastes are supplied  
355 to the M4 crypts and recycled by the symbiotic *Burkholderia* (29). We propose that the  
356 symbiont-mediated midgut closure, in conjunction with the CR and the unique digestive  
357 system, plays a significant role to stabilize the specific host-symbiont interaction in the bean  
358 bug.

359 The inoculation tests with colonization-defective mutants (Fig. 6c-f) suggest how the  
360 midgut closure is triggered by the symbiont. First, the absence of the midgut closure by the  
361 *fliC::Tn5* mutant that cannot pass through the CR, indicates that passage through this  
362 channel and/or M4 colonization is necessary to trigger the closure but that it cannot be

363 triggered by bacteria that are located at the M3-side of the CR. Second, the results of the  
364 colonization-defective mutants *purl::Tn5*,  $\Delta waaF$ , and  $\Delta phaB$  suggest that a weak  
365 colonization of the crypts is sufficient to trigger the midgut closure. Although the molecular  
366 mechanism of the midgut closure remains totally unknown, it appears likely that the bean  
367 bug recognizes the *Burkholderia* symbiont either in the CR or in the M4 by epithelial cells  
368 in a dose-dependent manner. In the legume-*Rhizobium* system, a lipochito-oligosaccharide  
369 (Nod factor) triggers the nodule formation (44). In the case of the bobtail squid, a  
370 peptidoglycan fragment, tracheal cytotoxin (TCT), derived from *Vibrio fischeri* alters  
371 morphogenesis of the light organ (45, 46). It is notable that in both cases, the host organisms  
372 recognize symbiont-associated molecular patterns via immune related receptors to trigger a  
373 developmental response (44, 47). Gut immunity genes have been reported in *R. pedestris*  
374 (48, 49), which may be involved in the here described symbiont-dependent morphogenesis  
375 in this insect. The bean bug is an ideal experimental system, where reverse genetic  
376 approaches have been established in both the host and in the symbiotic *Burkholderia* (25).  
377 Transcriptomic analyses of the CR during the closure, followed by RNAi screening, and  
378 identification of bacterial compounds triggering midgut closure in the absence of live  
379 bacteria, could be a strategy leading towards the understanding of the molecular basis  
380 underlying the symbiont-triggered morphogenesis in the bean bug.

381 We recently demonstrated that some non-symbiotic species of the genus *Burkholderia*  
382 and its outgroup *Pandoraea* can pass through the CR and stably but partially accommodate  
383 in the midgut crypts. Moreover, this colonization is beneficial for the host survival and  
384 development (36). Notably, while *E. coli* and *C. taiwanensis* showed neither M4  
385 colonization nor induction of the midgut closure (Fig. 6g and h), *B. fungorum* and *P.*

386 *norimbergensis* colonized the midgut crypts and induced the closure (Fig. 6i and j),  
387 suggesting that the microbial factors triggering the morphological alteration are conserved  
388 in this bacterial lineage. This reveals a potential drawback of the midgut closure mechanism  
389 because when induced by non-symbiotic species, it can restrict the access of the native  
390 symbiont to the M4 region if the symbiont is not present in the first infection event.  
391 However, these non-symbionts are rarely detected in natural populations of the bean bug (24,  
392 30, 50). Considering that the symbiotic *Burkholderia*, non-symbiotic *Burkholderia* and  
393 *Pandora* are very common bacterial groups in soil environments and frequently detected  
394 together (51-53), it is plausible that, in natural environments, these non-symbiotic species  
395 are usually ingested together with symbiotic *Burkholderia* and are then outcompeted by the  
396 native symbiont inside the midgut crypts (36), which ensures the specific association in  
397 natural populations of the bean bug.

398 Bottlenecks imposed on symbiont populations during their transmission or acquisition  
399 by the host are thought to strongly affect the population structure and evolution of  
400 symbionts (54). Such bottlenecks have been well described in insect symbioses with vertical  
401 transmission. These bottlenecks are large but vary from hundreds or thousands to several  
402 millions of symbiont cells transferred from mother to offspring, depending on the insect  
403 host and the specific transmission mode (54-57). On the contrary, in the few previously  
404 characterized symbioses without vertical transmission, symbionts seem to be selected from  
405 the environment in much smaller numbers; experimental studies on the legume-*Rhizobium*  
406 and squid-*Vibrio* model systems revealed that only a few symbiont cells (mostly only one  
407 bacterial cell) initiate the colonization, regardless of symbiont density in the environment  
408 (58, 59), suggesting a drastic partner choice in the initial stage of the infection. Relative

409 large bottlenecks during vertical transmission seem to be compatible with the fact that the  
410 symbiont lineage has been pre-selected efficiently in the previous generations of the host  
411 while the very narrow bottlenecks in environmental transmission modes might be required  
412 to cope with the extreme richness of microbes in the environment. However, unlike the  
413 legume and squid model systems, we determined a symbiont infection bottleneck of about  
414 4000 cells in *R. pedestris*, indicating a milder sorting, at least in the initial infection stage.  
415 Thus, the bean bug seems to adopt a different strategy than legumes and the squid and  
416 enables a range of bacteria, including some non-symbiont species, to pass the gate of the  
417 symbiotic organ (*i.e.* the CR). However, it applies then a severe selection inside the crypts  
418 of the symbiotic organ where non-symbiotic bacteria are very efficiently outcompeted by  
419 symbiont species (36).

420         The CR is widely conserved among diverse stinkbug species that harbor gut symbiotic  
421 bacteria in midgut crypts (33), including the *Bukholderia*-associated coreoid and lygaeoid  
422 species and members of the superfamily Pentatomoidea that vertically transmit  
423 gamma-proteobacterial symbionts. As the risk of contamination is a common issue in these  
424 gut symbiotic systems, it is plausible that the midgut closure after symbiont colonization is  
425 prevalent among the stink bug species. In the case of members of the Plataspidae and  
426 Urostylididae families belonging to the Pentatomoidea superfamily, the M3 and M4B are  
427 only joint by a thin connective tissue in adult insects (33, 60-62), suggesting that the CR is  
428 indeed closed and completely disconnected from the M3 after symbiont infection in these  
429 species. However, in case of the brown-winged green bug *Plautia stali*, the CR becomes  
430 looser after the 5<sup>th</sup> instar stage is reached and a food coloring can pass through from M3 to  
431 M4 (63). Thus, a morphological diversity of the CR exists among stinkbug species and may

432 reflect a functional difference of this organ. This potential divergence requires  
433 comprehensive comparative analyses between different stinkbug species.

434 Recent microbiome analyses have revealed that a number of animals possess diverse  
435 but highly specialized microbiota in their gut, which are maintained by various  
436 physiochemical, molecular, and structural mechanisms. In human gut microbiota, mucus  
437 layers containing specific polysaccharides and antimicrobial peptides (AMPs) control the  
438 microbiota and facilitate specific colonization of *Bacteroides* and *Acinatobacter* in colon  
439 crypts (64). In termites and honey bees, the hypoxia condition of the gut lumen remarkably  
440 contributes to shape their specific microbiota (15, 65, 66). In *Drosophila*, immune-related  
441 AMPs and reactive oxygen species limit the growth of pathogenic bacteria and play a  
442 significant role to establish its indigenous gut microbiota (67, 68). A more extreme case is  
443 found in the Sonoran Desert turtle ant, wherein a proventriculus valve located between the  
444 foregut and midgut filters out bacteria and keeps an exclusively specific microbiota in the  
445 midgut (69). Among these diverse mechanisms, the midgut closure reported here is an  
446 additional and unique mechanism to maintain the population of a specific bacterial partner  
447 and prevent chronic contamination with unwanted microbes. Our findings expand the  
448 understanding of how animals sustain specific gut symbiosis.

449

#### 450 **Acknowledgements**

451 We thank H. Ooi (AIST) for technical assistance. Part of the fluorescence microscopy was  
452 performed at the Imagerie-Gif facilities ([http://www.i2bc.paris-saclay.  
453 fr/spip.php?rubrique184](http://www.i2bc.paris-saclay.fr/spip.php?rubrique184)). This study was supported by the JSPS-CNRS Bilateral Open  
454 Partnership Joint Research Project to YK and PM, the Ministry of Education, Culture,

455 Sports, Science and Technology (MEXT) KAKENHI to YK (18KK0211), and the JSPS  
456 Research Fellowship for Young Scientists to TO (20170267 and 19J01106) and SJ  
457 (201911493).

458

459 **Author contributions**

460 YK, TO and PM designed the study. YK, TO and SJ performed inoculation tests, antibiotic  
461 treatments, and microscopy observations. TO and PM measured morphological change of gut  
462 parts and bottleneck of symbiont infection. YK and PM wrote the manuscript.

463

464 **Competing interests**

465 The authors declare that they have no competing interests.

466

467 **References**

- 468 1. Gilbert SF, Epel D. *Ecological developmental biology: integrating epigenetics,*  
469 *medicine, and evolution.* Sunderland, MA: Sinauer Associates Inc, 2009.
- 470 2. Nyholm SV, McFall-Ngai M. The winnowing: establishing the squid-*Vibrio* symbiosis.  
471 *Nat Rev Microbiol.* 2004; 2: 632-642.
- 472 3. Kondorosi E, Mergaert P, Kereszt A. A paradigm for endosymbiotic life: cell  
473 differentiation of *Rhizobium* bacteria provoked by host plant factors. *Ann Rev*  
474 *Microbiol.* 2013; 67: 611-628.
- 475 4. Sommer F, Backhed F. The gut microbiota-masters of host development and  
476 physiology. *Nat Rev Microbiol.* 2013; 11: 227-238.
- 477 5. Broderick NA, Buchon N, Lemaitre B. Microbiota-induced changes in *Drosophila*  
478 *melanogaster* host gene expression and gut morphology. *MBio.* 2014; 5:  
479 e01117-01114.
- 480 6. Vacheron J, Desbrosses G, Bouffaud M-L, Touraine B, Moënne-Loccoz Y, Muller D  
481 *et al.* Plant growth-promoting rhizobacteria and root system functioning. *Front Plant*  
482 *Sci.* 2013; 4: 356.
- 483 7. Shikuma NJ, Pilhofer M, Weiss GL, Hadfield MG, Jensen GJ, Newman DK. Marine  
484 tubeworm metamorphosis induced by arrays of bacterial phage tail-like structures.  
485 *Science.* 2014; 343: 529-533.
- 486 8. Shikuma NJ, Antoshechkin I, Medeiros JM, Pilhofer M, Newman DK. Stepwise  
487 metamorphosis of the tubeworm *Hydroides elegans* is mediated by a bacterial inducer  
488 and MAPK signaling. *Proc Natl Acad Sci USA.* 2016; 113: 10097-10102.
- 489 9. Ericson CF, Eisenstein F, Medeiros JM, Malter KE, Cavalcanti GS, Zeller RW *et al.* A

- 490 contractile injection system stimulates tubeworm metamorphosis by translocating a  
491 proteinaceous effector. *eLife*. 2019; 8: e46845.
- 492 10. Alegado RA, Brown LW, Cao S, Dermenjian RK, Zuzow R, Fairclough SR *et al.* A  
493 bacterial sulfonolipid triggers multicellular development in the closest living relatives  
494 of animals. *eLife*. 2012; 1: e00013.
- 495 11. Buchner P. *Endosymbiosis of animals with plant microorganism*. New York:  
496 Interscience, 1965.
- 497 12. Kikuchi Y. Endosymbiotic bacteria in insects: their diversity and culturability.  
498 *Microbes Environ*. 2009; 24: 195-204.
- 499 13. Moran NA, McCutcheon JP, Nakabachi A. Genomics and evolution of heritable  
500 bacterial symbionts. *Annu Rev Genet*. 2008; 42: 165-190.
- 501 14. Douglas AE. Lessons from studying insect symbioses. *Cell Host Microbe*. 2011; 10:  
502 359-367.
- 503 15. Utami YD, Kuwahara H, Murakami T, Morikawa T, Sugaya K, Kihara K *et al.*  
504 Phylogenetic diversity and single-cell genome analysis of “*Melainabacteria*”, a  
505 non-photosynthetic cyanobacterial group, in the termite gut. *Microbes Environ*. 2018;  
506 33: 50-57.
- 507 16. Hosokawa T, Kikuchi Y, Shimada M, Fukatsu T. Symbiont acquisition alters  
508 behaviour of stinkbug nymphs. *Biol Lett*. 2008; 4: 45-48.
- 509 17. Werren JH, Baldo L, Clark ME. *Wolbachia*: master manipulators of invertebrate  
510 biology. *Nat Rev Microbiol*. 2008; 6: 741.
- 511 18. Feldhaar H. Bacterial symbionts as mediators of ecologically important traits of insect  
512 hosts. *Ecol Entomol*. 2011; 36: 533-543.

- 513 19. Kikuchi Y, Hayatsu M, Hosokawa T, Nagayama A, Tago K, Fukatsu T.  
514 Symbiont-mediated insecticide resistance. Proc Natl Acad Sci USA. 2012; 109:  
515 8618-8622.
- 516 20. Flórez LV, Biedermann PH, Engl T, Kaltenpoth M. Defensive symbioses of animals  
517 with prokaryotic and eukaryotic microorganisms. Nat Prod Rep. 2015; 32: 904-936.
- 518 21. Tsuchida T. Molecular basis and ecological relevance of aphid body colors. Curr Opin  
519 Insect Sci. 2016; 17: 74-80.
- 520 22. Anbutsu H, Moriyama M, Nikoh N, Hosokawa T, Futahashi R, Tanahashi M *et al.*  
521 Small genome symbiont underlies cuticle hardness in beetles. Proc Natl Acad Sci  
522 USA. 2017; 114: E8382-E8391.
- 523 23. Itoh H, Tago K, Hayatsu M, Kikuchi Y. Detoxifying symbiosis: microbe-mediated  
524 detoxification of phytotoxins and pesticides in insects. Nat Prod Rep. 2018; 35:  
525 434-454.
- 526 24. Kikuchi Y, Meng XY, Fukatsu T. Gut symbiotic bacteria of the genus *Burkholderia* in  
527 the broad-headed bugs *Riptortus clavatus* and *Leptocorisa chinensis* (Heteroptera:  
528 Alydidae). Appl Environ Microbiol. 2005; 71: 4035-4043.
- 529 25. Takeshita K, Kikuchi Y. *Riptortus pedestris* and *Burkholderia* symbiont: an ideal  
530 model system for insect-microbe symbiotic associations. Res Microbiol. 2016; 168:  
531 175-187.
- 532 26. Takeshita K, Tamaki H, Ohbayashi T, Meng XY, Sone T, Mitani Y *et al.* *Burkholderia*  
533 *insecticola* sp. nov., a gut symbiotic bacterium of the bean bug *Riptortus pedestris*. *Int*  
534 *J Syst Evol Microbiol*. 2018; 68: 2370-2374.
- 535 27. Kaltenpoth M, Flórez LV. Versatile and dynamic symbioses between insects and

- 536 *Burkholderia* bacteria. Annu Rev Entomol. 2019; epub ahead of print 8 October 2019;  
537 doi: 10.1146/annurev-ento-011019-025025.
- 538 28. Kikuchi Y, Fukatsu T. Live imaging of symbiosis: spatiotemporal infection dynamics  
539 of a GFP-labelled *Burkholderia* symbiont in the bean bug *Riptortus pedestris*. Mol  
540 Ecol. 2014; 23: 1445-1456.
- 541 29. Ohbayashi T, Futahashi R, Terashima M, Barrière Q, Lamouche F, Takeshita K *et al.*  
542 Comparative cytology, physiology and transcriptomics of *Burkholderia insecticola* in  
543 symbiosis with the bean bug *Riptortus pedestris* and in culture. ISME J. 2019; 13:  
544 1469-1483.
- 545 30. Kikuchi Y, Hosokawa T, Fukatsu T. Insect-microbe mutualism without vertical  
546 transmission: a stinkbug acquires a beneficial gut symbiont from the environment  
547 every generation. Appl Environ Microbiol. 2007; 73: 4308-4316.
- 548 31. Kikuchi Y, Hosokawa T, Fukatsu T. Specific developmental window for establishment  
549 of an insect-microbe gut symbiosis. Appl Environ Microbiol. 2011; 77: 4075-4081.
- 550 32. Bahram M, Hildebrand F, Forslund SK, Anderson, JL, Soudzilovskaia NA, Bodegom  
551 PM *et al.* Structure and function of the global topsoil microbiome. Nature. 2018; 560:  
552 233-237.
- 553 33. Ohbayashi T, Takeshita K, Kitagawa W, Nikoh N, Koga R, Meng XY *et al.* Insect's  
554 intestinal organ for symbiont sorting. Proc Natl Acad Sci USA. 2015; 112:  
555 E5179-E5188.
- 556 34. Kinoshita Y, Kikuchi Y, Mikami N, Nakane D, Nishizaka T. Unforeseen swimming and  
557 gliding mode of an insect gut symbiont, *Burkholderia* sp. RPE64, with wrapping of  
558 the flagella around its cell body. ISME J. 2018; 12: 838-848.

- 559 35. Raina JB, Fernandez V, Lambert B, Stocker R, Seymour JR. The role of microbial  
560 motility and chemotaxis in symbiosis. *Nat Rev Microbiol.* 2019; 17: 284-294.
- 561 36. Itoh H, Jang S, Takeshita K, Ohbayashi T, Ohnishi N, Meng XY *et al.* Host-symbiont  
562 specificity determined by microbe-microbe competition in an insect gut. *Proc Natl*  
563 *Acad Sci USA.* 2019; 116: 22673-22682.
- 564 37. Norris MH, Kang Y, Wilcox B, Hoang TT. Stable, site-specific fluorescent tagging  
565 constructs optimized for *Burkholderia* species. *Appl Environ Microbiol.* 2010; 76:  
566 7635-7640.
- 567 38. Vergunst AC, Meijer AH, Renshaw SA, O'Callaghan D. *Burkholderia cenocepacia*  
568 creates an intramacrophage replication niche in zebrafish embryos, followed by  
569 bacterial dissemination and establishment of systemic infection. *Infect Immun.* 2010;  
570 78: 1495-1508.
- 571 39. Kim JK, Kim NH, Jang HA, Kikuchi Y, Kim CH, Fukatsu T *et al.* Specific midgut  
572 region controlling the symbiont population in an insect-microbe gut symbiotic  
573 association. *Appl Environ Microbiol.* 2013; 79: 7229-7233.
- 574 40. Kim JK, Jang HA, Won YJ, Kikuchi Y, Heum Han S, Kim CH *et al.* Purine  
575 biosynthesis-deficient *Burkholderia* mutants are incapable of symbiotic  
576 accommodation in the stinkbug. *ISME J.* 2014; 8: 552-563.
- 577 41. Kim JK, Jang HA, Kim MS, Cho JH, Lee JB, Lorenzo FD *et al.* The  
578 lipopolysaccharide core oligosaccharide of *Burkholderia* plays a critical role in  
579 maintaining a proper gut symbiosis with the bean bug *Riptortus pedestris*. *J Biol*  
580 *Chem.* 2017; 292: 19226-19237.
- 581 42. Kim JK, Won YJ, Nikoh N, Nakayama H, Han SH, Kikuchi Y *et al.* Polyester

- 582 synthesis genes associated with stress resistance are involved in an insect-bacterium  
583 symbiosis. Proc Natl Acad Sci USA. 2013; 110: E2381-2389.
- 584 43. Yasunaga T, Takai M, Yamashita I, Kawamura M, Kawasaki T. *A Field Guide to*  
585 *Japanese Bugs*. Zenkoku Nousei Kyouiku Kyokai: Tokyo, Japan, 1993.
- 586 44. Zipfel C, Oldroyd GE. Plant signalling in symbiosis and immunity. Nature. 2017; 543:  
587 328-336.
- 588 45. Koropatnick TA, Engle JT, Apicella MA, Stabb EV, Goldman WE, McFall-Ngai, MJ.  
589 Microbial factor-mediated development in a host-bacterial mutualism. Science. 2004;  
590 306: 1186-1188.
- 591 46. Adin DM, Engle, JT, Goldman WE, McFall-Ngai, MJ, Stabb, EV. Mutations in *ampG*  
592 and lytic transglycosylase genes affect the net release of peptidoglycan monomers  
593 from *Vibrio fischeri*. J Bacteriol. 2009; 191: 2012-2022.
- 594 47. Chu H, Mazmanian SK. Innate immune recognition of the microbiota promotes  
595 host-microbial symbiosis. Nat Immunol. 2013; 14: 668-675.
- 596 48. Kim JK, Lee JB, Jang HA, Han YS, Fukatsu T, Lee BL. Understanding regulation of  
597 the host-mediated gut symbiont population and the symbiont-mediated host immunity  
598 in the *Riptortus-Burkholderia* symbiosis system. Dev Comp Immunol. 2016; 64:  
599 75-81.
- 600 49. Park KE, Jang SH, Lee J, Lee SA, Kikuchi Y, Seo YS *et al*. The roles of antimicrobial  
601 peptide, rip-thanatin, in the midgut of *Riptortus pedestris*. Dev Comp Immunol. 2017;  
602 78: 83-90.
- 603 50. Kikuchi Y, Hosokawa T, Fukatsu T. An ancient but promiscuous host-symbiont  
604 association between *Burkholderia* gut symbionts and their heteropteran hosts. ISME J.

- 605 2011; 5: 446-460.
- 606 51. Itoh H, Navarro R, Takeshita K, Tago K, Hayatsu M, Hori T *et al.* Bacterial  
607 population succession and adaptation affected by insecticide application and soil  
608 spraying history. *Front Microbiol.* 2014; 5: 457.
- 609 52. Itoh H, Hori T, Sato Y, Nagayama A, Tago K, Hayatsu M *et al.* Infection dynamics of  
610 insecticide-degrading symbionts from soil to insects in response to insecticide  
611 spraying. *ISME J.* 2018; 12: 909-920.
- 612 53. Stopnisek N, Bodenhausen N, Frey B, Fierer N, Eberl L, Weisskopf L. Genus-wide  
613 acid tolerance accounts for the biogeographical distribution of soil *Burkholderia*  
614 populations. *Environ Microbiol.* 2014; 16: 1503-12.
- 615 54. Campbell MA, Łukasik P, Meyer MC, Buckner M, Simon C, Veloso C *et al.* Changes  
616 in endosymbiont complexity drive host-level compensatory adaptations in cicadas.  
617 *mBio.* 2018;9: e02104-18.
- 618 55. Mira A, Moran NA. Estimating population size and transmission bottlenecks in  
619 maternally transmitted endosymbiotic bacteria. *Microb Ecol.* 2002; 44: 137-143.
- 620 56. Kaltenpoth M, Goettler W, Koehler S, Strohm E. Life cycle and population dynamics  
621 of a protective insect symbiont reveal severe bottlenecks during vertical transmission.  
622 *Evol Ecol.* 2010; 24: 463–477.
- 623 57. Hosokawa T, Kikuchi Y, Fukatsu T. How many symbionts are provided by mothers,  
624 acquired by offspring, and needed for successful vertical transmission in an obligate  
625 insect-bacterium mutualism? *Mol Ecol.* 2007; 16: 5316-5325.
- 626 58. Wollenberg MS, Ruby EG. Population structure of *Vibrio fischeri* within the light  
627 organs of *Euprymna scolopes* squid from two Oahu (Hawaii) populations. *Appl*

- 628 Environ Microbiol. 2009; 75: 193-202.
- 629 59. Gage DJ. Analysis of infection thread development using GFP- and DsRed-expressing  
630 *Sinorhizobium meliloti*. J Bacteriol. 2002; 184: 7042-7046.
- 631 60. Schneider G. Beiträge zur Kenntnis der symbiontischen Einrichtungen der  
632 Heteropteren. Z Morphol O'kol Tiere. 1940; 36:565-644.
- 633 61. Fukatsu T, Hosokawa T. Capsule-transmitted gut symbiotic bacterium of the Japanese  
634 common plataspid stinkbug, *Megacopta punctatissima*. Appl Environ Microbiol.  
635 2002; 68: 389-396.
- 636 62. Kaiwa N, Hosokawa T, Nikoh N, Tanahashi M, Moriyama M, Meng XY *et al.*  
637 Symbiont-supplemented maternal investment underpinning host's ecological  
638 adaptation. Curr Biol. 2014; 24: 2465-2470.
- 639 63. Oishi S, Moriyama M, Koga R, Fukatsu T. Morphogenesis and development of  
640 midgut symbiotic organ of the stinkbug *Plautia stali* (Hemiptera: Pentatomidae).  
641 Zoological Lett. 2019; 5:16.
- 642 64. Donaldson GP, Lee SM, Mazmanian SK. Gut biogeography of the bacterial  
643 microbiota. Nat Rev Microbiol. 2016; 14: 20-32.
- 644 65. Brune A, Emerson D, Breznak JA. The termite gut microflora as an oxygen sink:  
645 microelectrode determination of oxygen and pH gradients in guts of lower and higher  
646 termites. Appl Environ Microbiol. 1995; 61: 2681-2687.
- 647 66. Zheng H, Powell JE, Steele MI, Dietrich C, Moran NA. Honeybee gut microbiota  
648 promotes host weight gain via bacterial metabolism and hormonal signaling. Proc  
649 Natl Acad Sci USA. 2017; 114: 4775-4780.
- 650 67. Buchon N, Broderick NA, Lemaitre B. Gut homeostasis in a microbial world: insights

- 651 from *Drosophila melanogaster*. Nat Rev Microbiol. 2013; 11: 615-626.
- 652 68. Lee WJ, Hase K. Gut microbiota-generated metabolites in animal health and disease.
- 653 Nat Chem Biol. 2014; 10: 416-424.
- 654 69. Lanan MC, Rodrigues PA, Agellon A, Jansma P, Wheeler DE. A bacterial filter
- 655 protects and structures the gut microbiome of an insect. ISME J. 2016; 10: 1866-1876.
- 656

657 **Figure legends**

658 **Fig. 1. Morphological alteration of the constricted region and M4B during symbiont**  
659 **colonization in 2<sup>nd</sup> instar nymphs of *R. pedestris*. (a-r)** A GFP-labelled *Burkholderia*  
660 symbiont was orally administered, and the posterior part of the midgut (M2-M4) was  
661 observed by epifluorescence microscopy, starting from the time of symbiont inoculation to  
662 72 hours after inoculation, just before the 3<sup>rd</sup> instar molting. Host nuclear DNA was stained  
663 by DAPI. The M4B is closed during symbiont infection **(a-h)** and reopened by backflow of  
664 symbiont cells during the colonization of M4 **(i-r)**. Abbreviations: M2, midgut second  
665 section; M3, midgut third section; M4, midgut fourth section with crypts (symbiotic organ);  
666 M4B, M4 bulb; H, hindgut. **(s)** Change of the CR width. While the CR width continuously  
667 increases in aposymbiotic insects, the CR becomes thinner during 12-18 hpi (arrow). This  
668 timing corresponds to the midgut closure event. **(t)** Change of the maximum M4B width.  
669 After the flow back of symbiont cells from M4 to M4B, occurring around 36-48 hpi, the  
670 M4B becomes bulbous. n = 5. Welch's *t*-test was performed between aposymbiotic and  
671 symbiotic insects (\*\* P < 0.05; \*\*\* P < 0.005).

672

673 **Fig. 2. Closing of the constricted region. (a)** At 24 h after inoculation, the CR and the  
674 M4B region are completely closed. **(b)** LSM observations reveal that epithelial cells of  
675 M4B are bulged at the luminal side and closed like a zipper during symbiont colonization.  
676 **(c)** At 72 h after inoculation, symbiont cells flow back into M4B, but never flow over into  
677 M3. **(d)** LSM observations indicate that the CR (arrowheads) is kept closed after the  
678 reopening of M4B. In **(a)** and **(c)**, host nuclei are stained by DAPI, shown in blue. In **(b)**  
679 and **(d)**, host nuclei and cytoskeleton are stained with SYTOX green (green) and phalloidin

680 (red), respectively.

681

682 **Fig. 3. The closure of the constricted region and M4B during symbiont colonization in**  
683 **3<sup>rd</sup> instar nymphs of *R. pedestris*.** (a) Infection scheme. (b-g) No morphological alteration  
684 in the M4B of aposymbiotic 2<sup>nd</sup> instar insects. Asterisks indicate the lumen of M4B. (h-m)  
685 A GFP-labelled *Burkholderia* symbiont was orally administered to aposymbiotic 3<sup>rd</sup> instar  
686 nymphs and their M4B morphogenesis was investigated. Merged fluorescence and DIC  
687 images are shown. Abbreviations are as in [Fig. 1](#).

688

689 **Fig. 4. The midgut closure prevents subsequent infections.** (a) Experimental set-up of  
690 re-inoculation of the *Burkholderia* symbiont. An RFP-labelled symbiont was orally  
691 administered at the 2<sup>nd</sup> instar stage. After the symbiont colonized the gut symbiotic organ  
692 and the nymphs were molted into the 3<sup>rd</sup> instar, a GFP-labelled symbiont was fed to the  
693 insects. (b and c) GFP-labelled symbionts are not able to enter the M4B and M4 regions  
694 anymore after the midgut closure following the initial infection. Observations were made 24  
695 h (b) and 48 h (c) after inoculation of the GFP-labelled symbiont. Whole gut images and  
696 LSM images of M3-M4B region are shown. While in the LSM images, GFP signals are  
697 detected in the lumen of the M3, no GFP is detected behind the CR. Abbreviations are as in  
698 [Fig. 1](#).

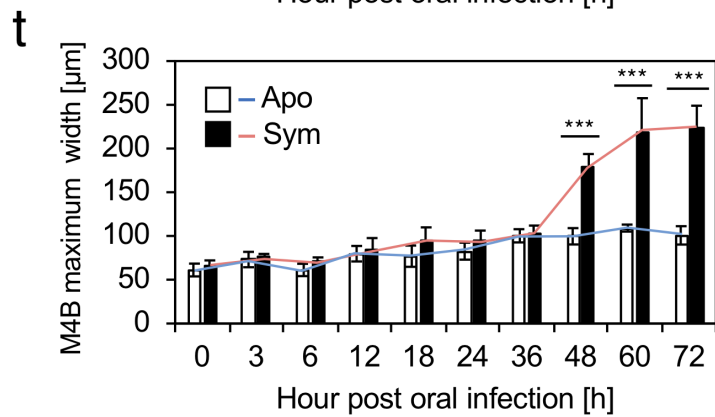
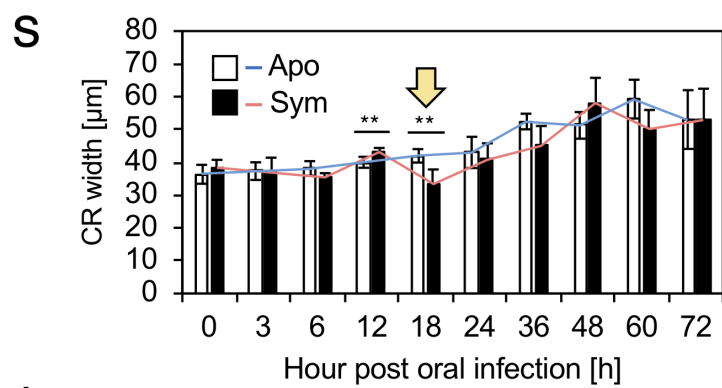
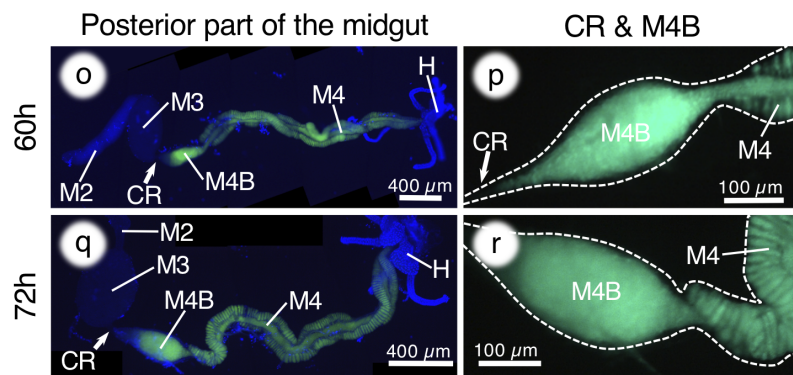
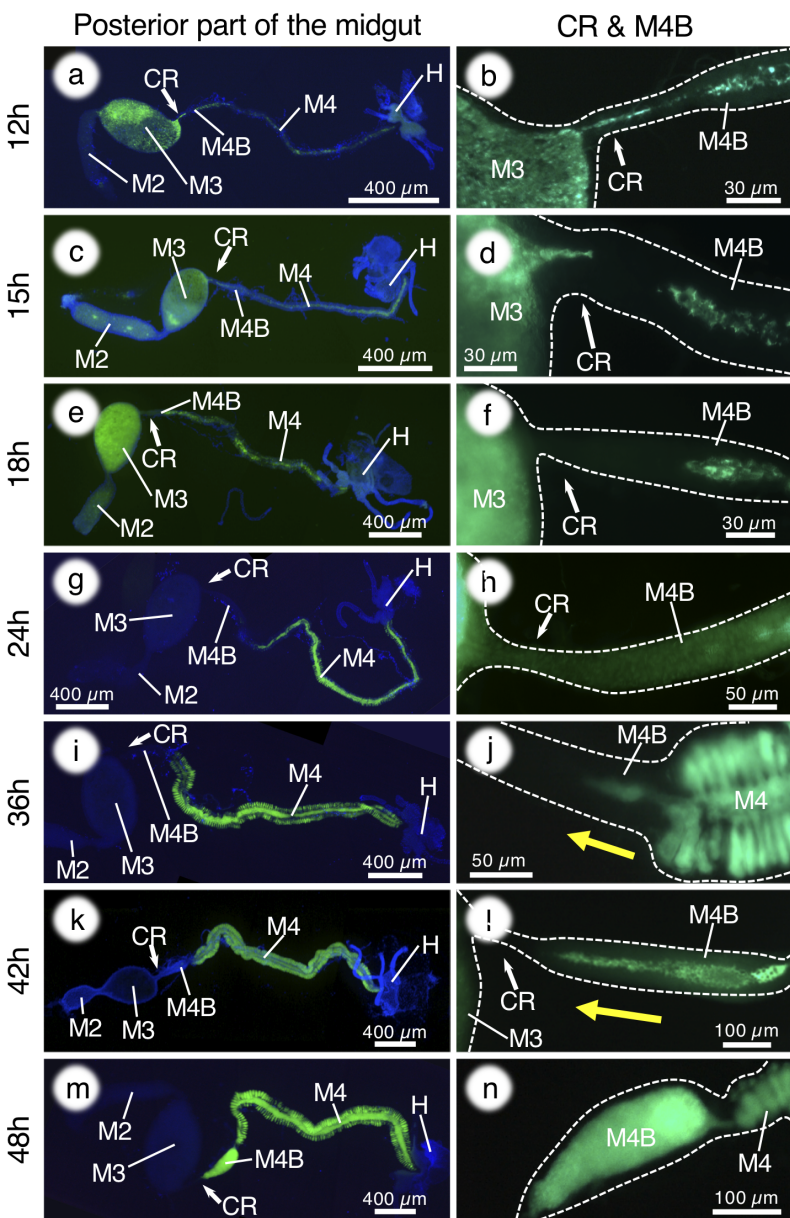
699

700 **Fig. 5. The midgut closure is irreversible.** (a) Infection schemes for three series of  
701 experiments. In the Cm-RFP control experiment, 2<sup>nd</sup> instar insects are kept aposymbiotic  
702 and fed with chloramphenicol (Cm) in the drinking water; after molting, these insects are

703 infected with the RFP strain. In the GFP-RFP control experiment, 2<sup>nd</sup> instar insects are  
704 infected with the GFP strain present in the drinking water and after molting, the 3<sup>rd</sup> instars  
705 are exposed to the RFP strain present in the drinking water. In the GFP-Cm-RFP experiment,  
706 2<sup>nd</sup> instar insects are infected with the GFP strain present in the drinking water; after 24 h,  
707 this drinking water is replaced by chloramphenicol-containing drinking water; the 3<sup>rd</sup> instars  
708 are then exposed to the RFP strain. In all infection schemes, the infection status was  
709 analyzed by dissection and microscopy in 3 dpi 2<sup>nd</sup> instar insects and in 3 dpi 3<sup>rd</sup> instar  
710 insects. **(b)** Infection status in 2<sup>nd</sup> instar insects. **(c)** Infection status in 3<sup>rd</sup> instar insects. In  
711 **(b)** and **(c)**, red and green fluorescence, DIC and merged images are shown. Note the  
712 “fluorescence” panels are merged images of red and green.

713

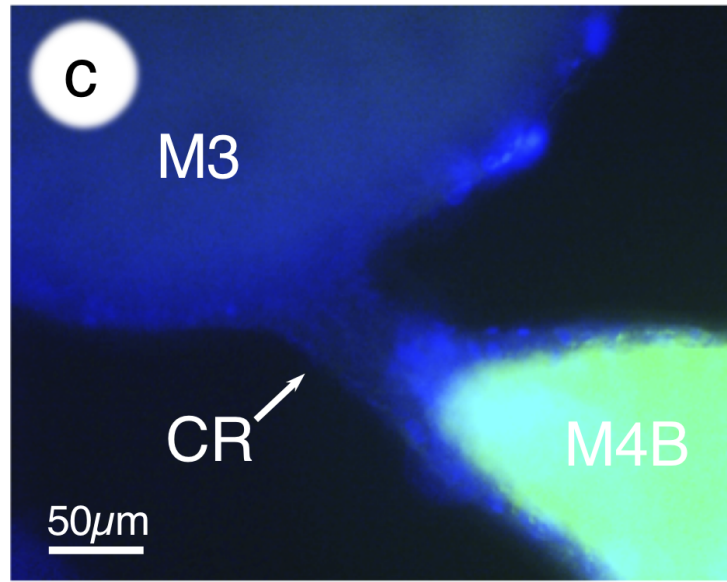
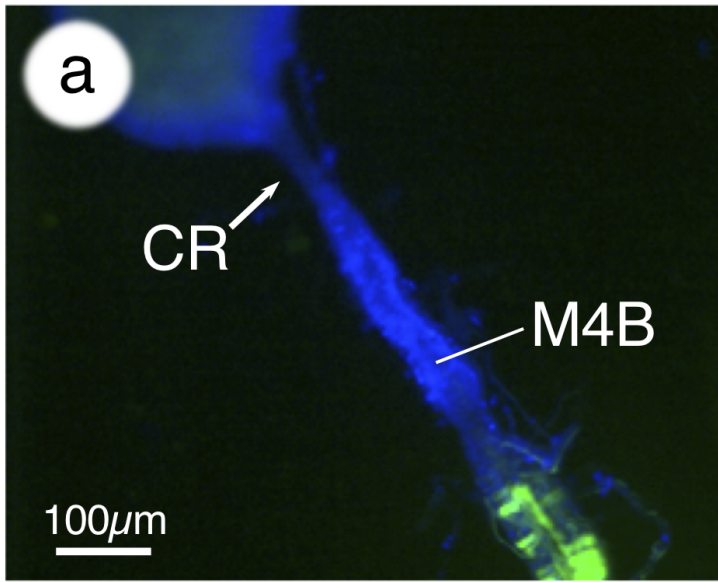
714 **Fig. 6. Midgut closure requires passage through the constricted region and crypt**  
715 **colonization.** **(a)** Infection scheme: 2<sup>nd</sup> instar insects were infected with different  
716 GFP-labelled strains and after molting, 3<sup>rd</sup> instars were infected with the wild type RFP  
717 symbiont to verify the occurrence or not of midgut closure triggered by the first inoculation.  
718 **(b-j)** Infection status of 3 dpi 3<sup>rd</sup> instar insects, analyzed by dissection and microscopy, after  
719 infection in the 2<sup>nd</sup> instar with the wild type **(b)**, the *fliC::Tn5* **(c)**, *purL::Tn5* **(d)**, *ΔwaaF* **(e)**  
720 and *ΔphaB* **(f)** mutants of *B. insecticola*, with *E. coli* **(g)** and *C taiwanensis* **(h)** that cannot  
721 pass through the CR, and with *B. fungorum* **(i)** and *P. norimbergensis* **(j)** that can pass  
722 through the CR and partially colonize the M4 crypts. In **(b-j)**, fluorescence images are  
723 shown. Note the fluorescence panels are merged images of red and green.



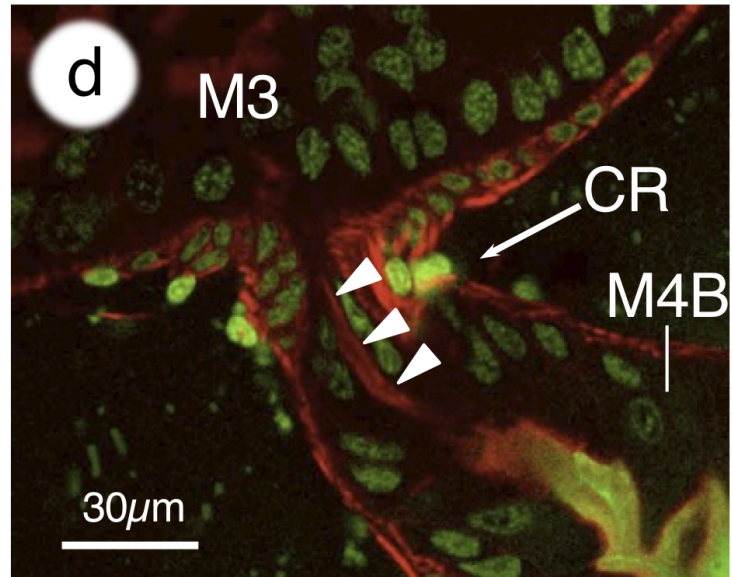
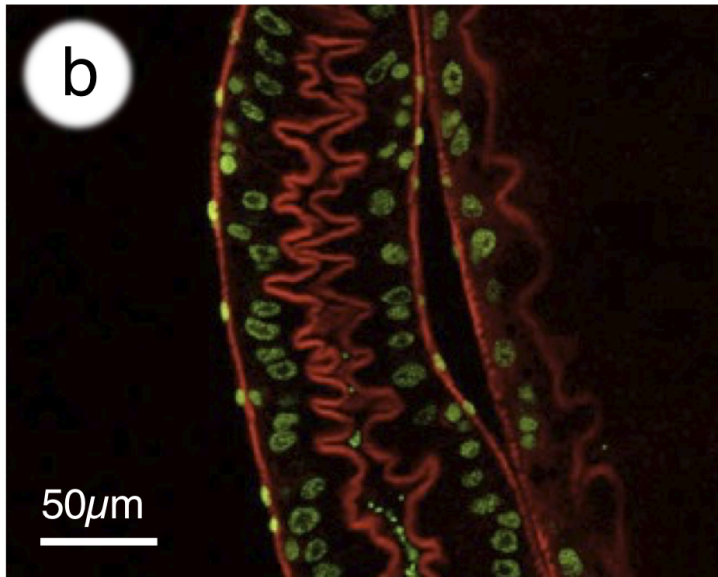
Fluorescent  
microscopy

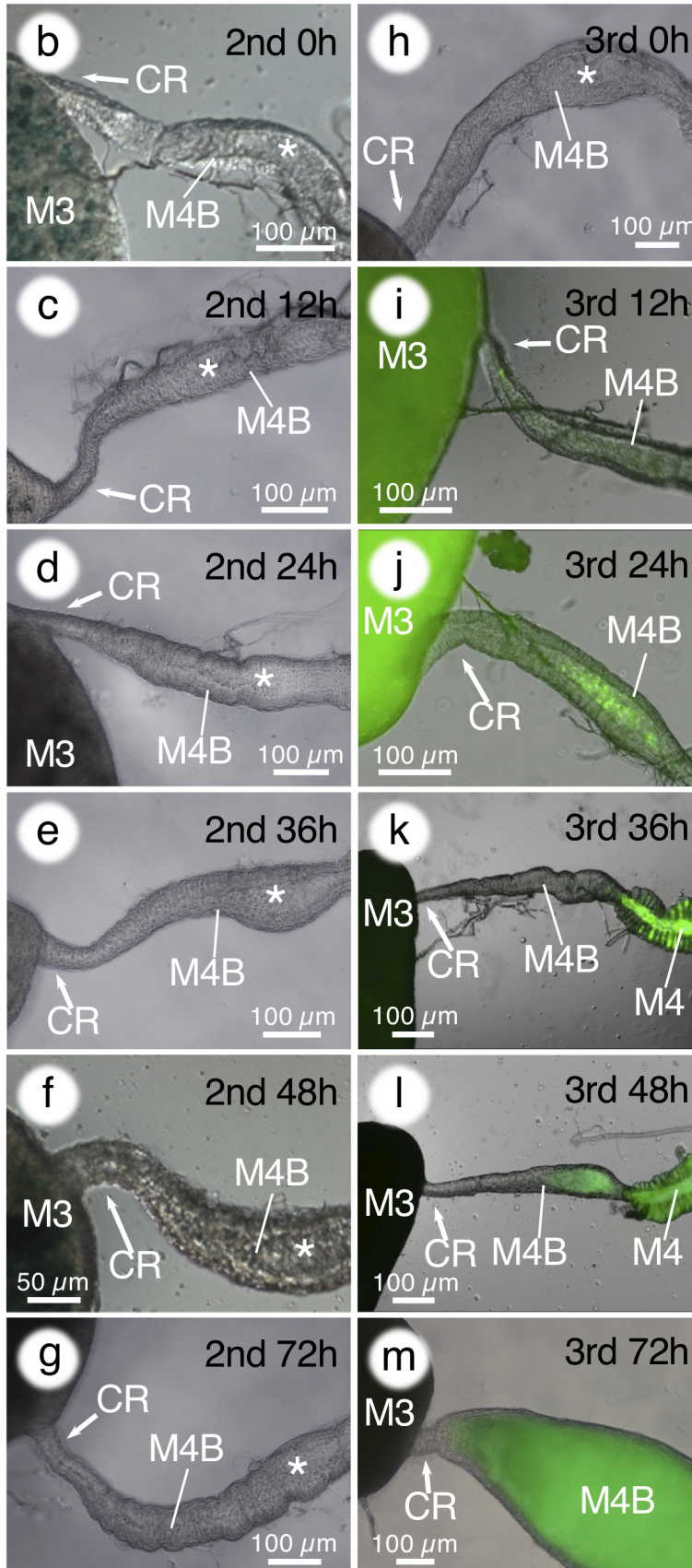
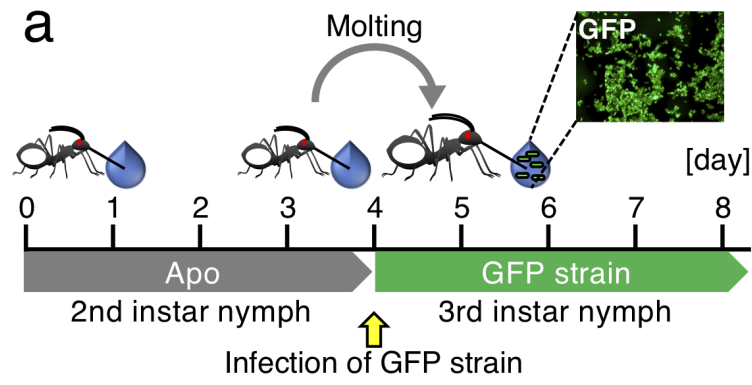
24h

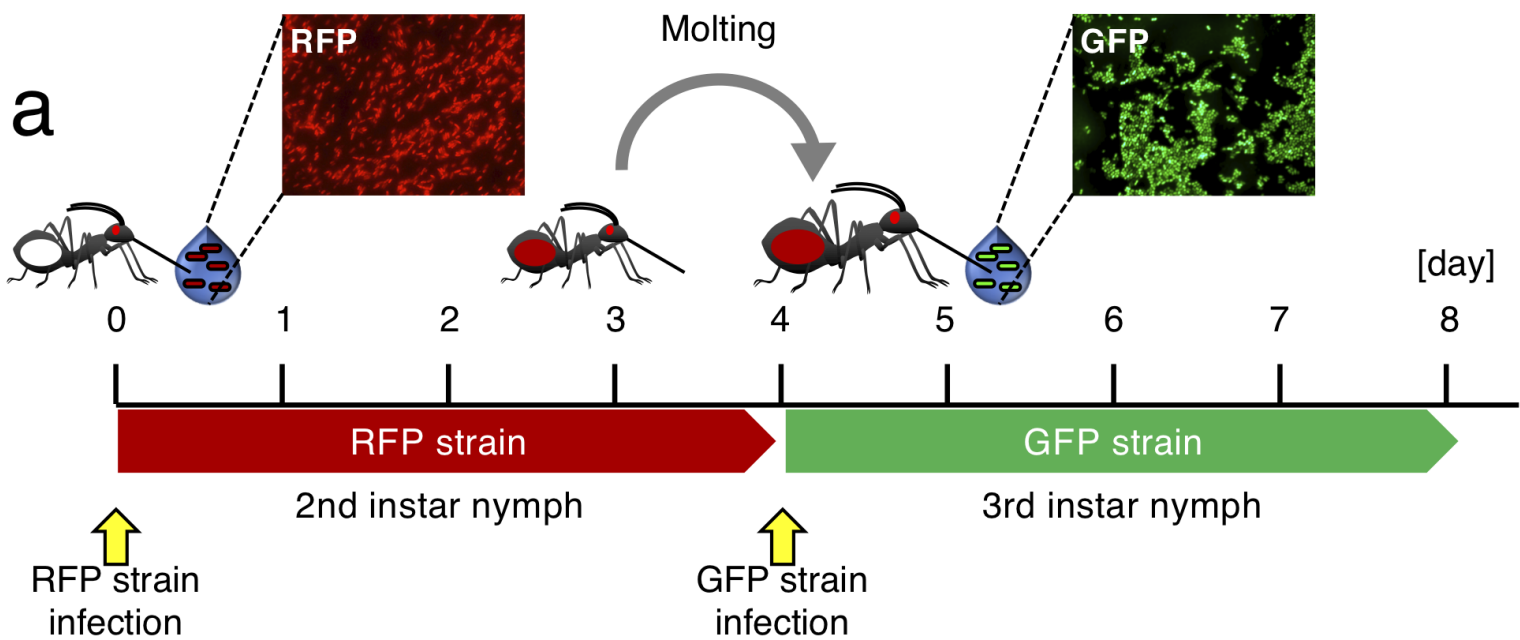
72h



LSM

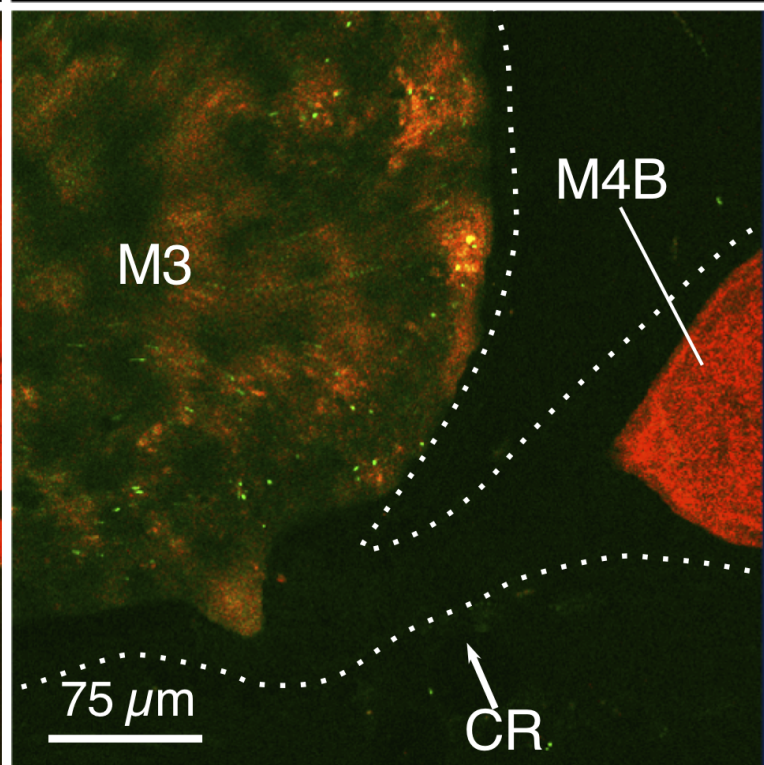
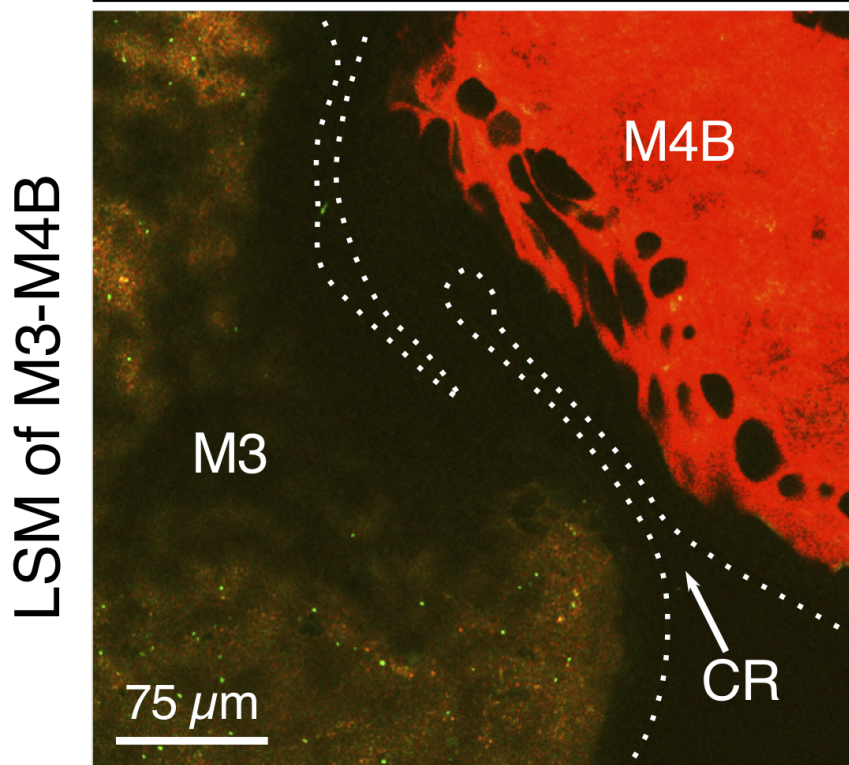
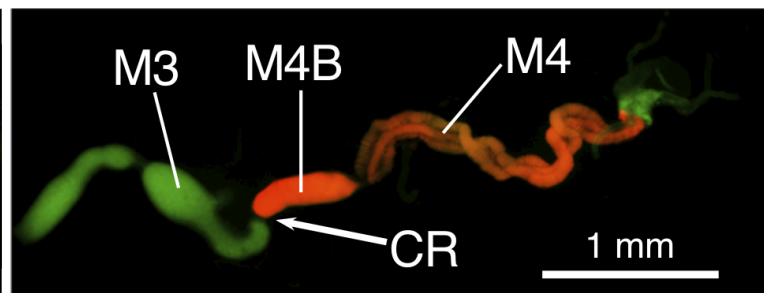
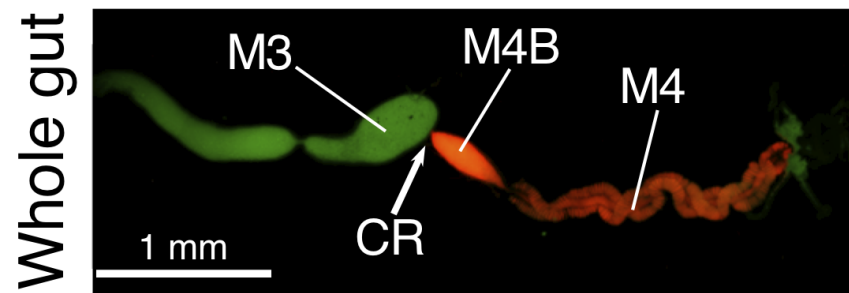


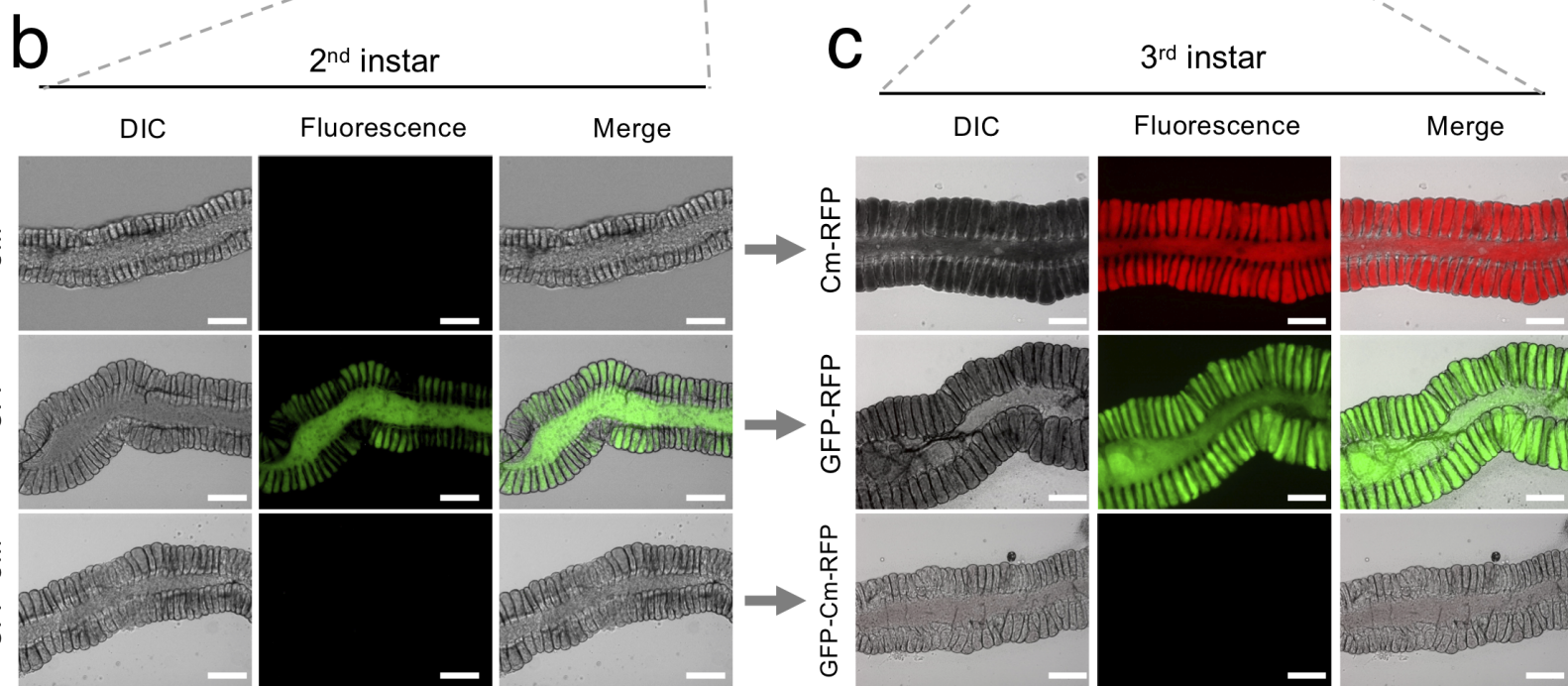
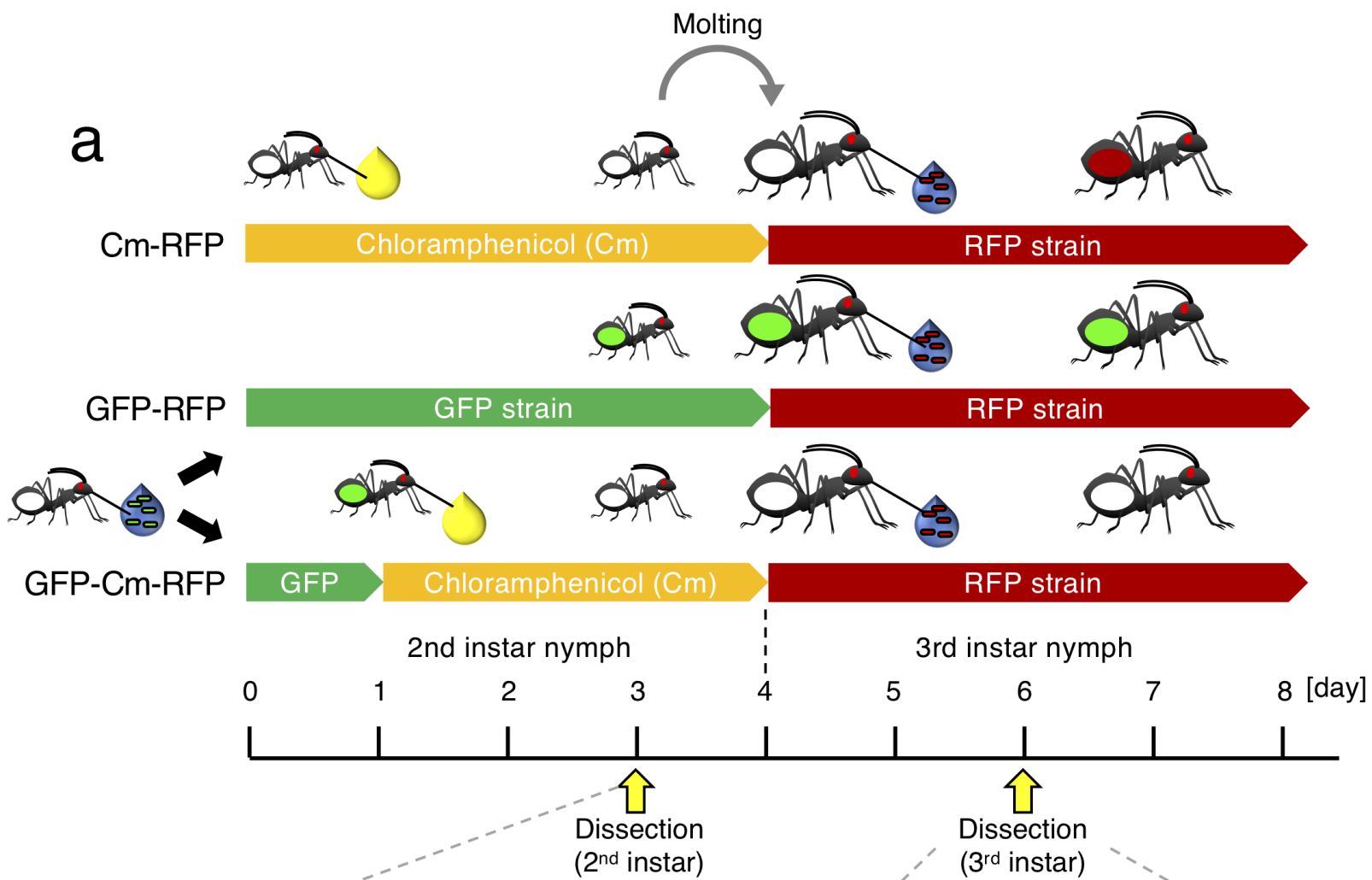




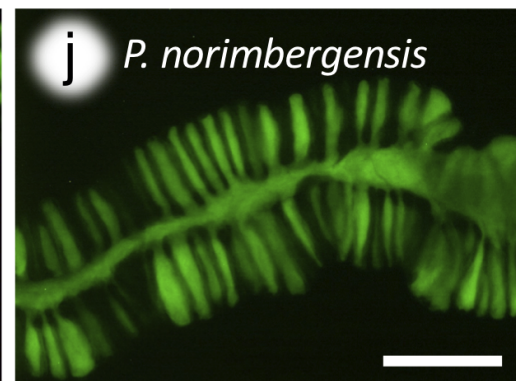
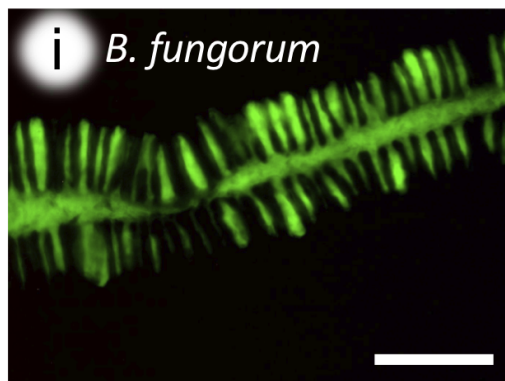
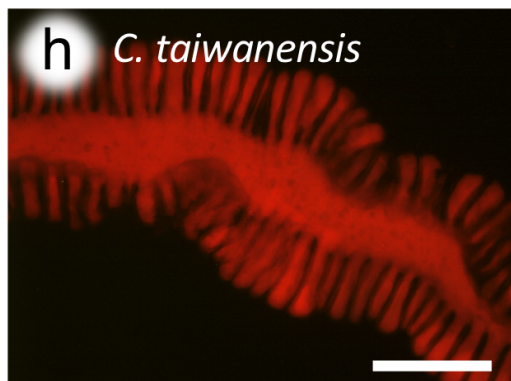
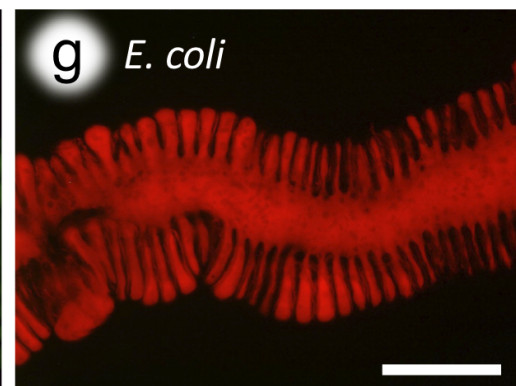
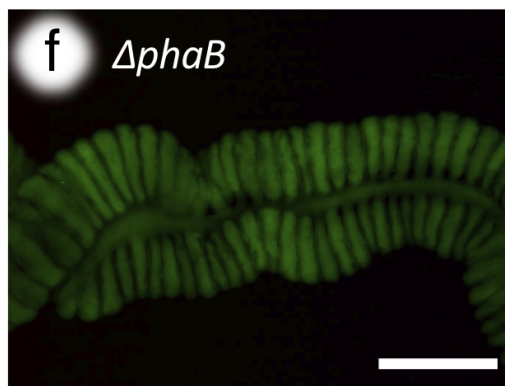
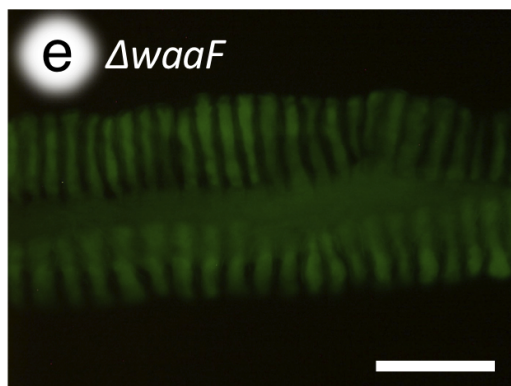
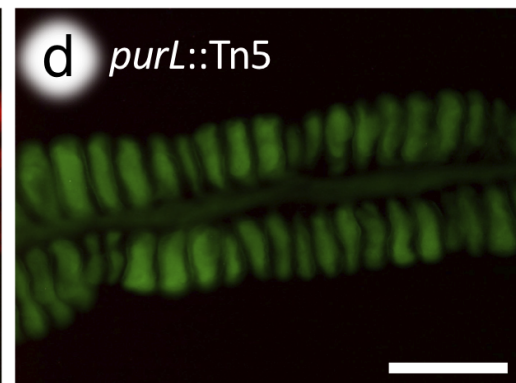
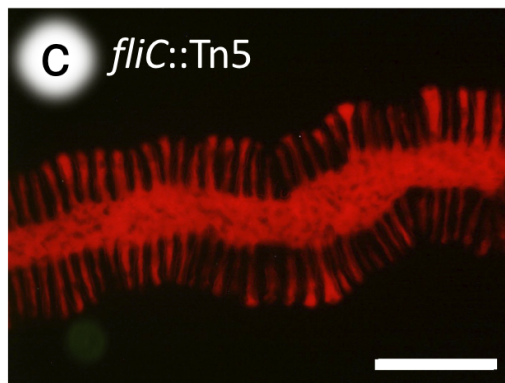
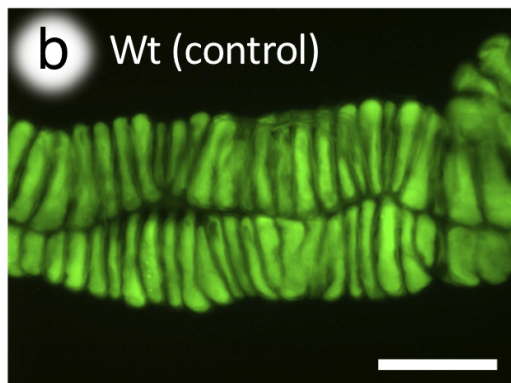
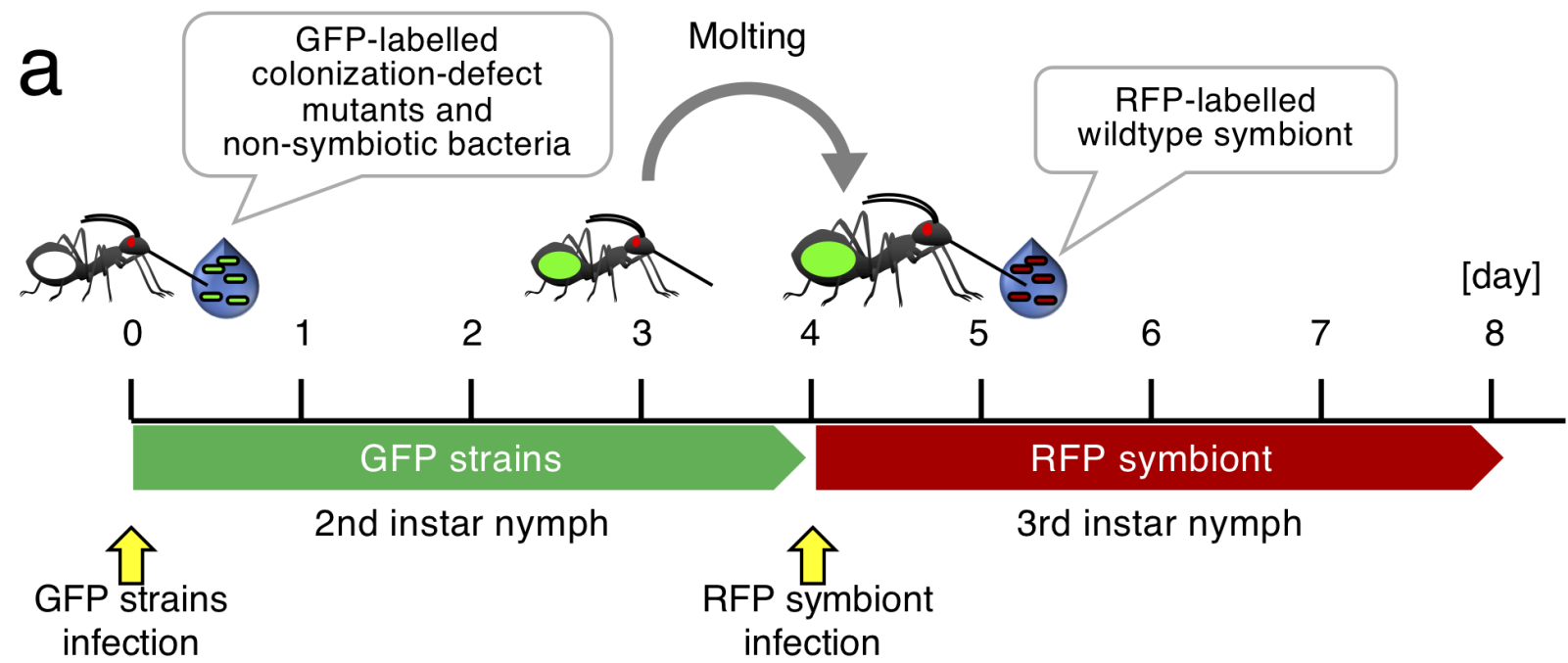
**b** 24 h post re-inoculation of GFP strain

**c** 48 h post re-inoculation of GFP strain





200  $\mu$ m



200  $\mu$ m

## SUPPLEMENTARY INFORMATION

### ***Burkholderia insecticola* triggers midgut closure in the bean bug *Riptortus pedestris* to prevent secondary bacterial infections of midgut crypts**

Yoshitomo Kikuchi, Tsubasa Ohbayashi, Seonghan Jang and Peter Mergaert

#### **Supplementary Materials and Methods**

##### **Microscopic observations of dissected symbiotic organs**

The insects administered with the GFP-labeled or RFP labelled strains were dissected in phosphate-buffered saline (PBS: 137 mM NaCl, 8.1 mM Na<sub>2</sub>HPO<sub>4</sub>, 2.7 mM KCl, 1.5 mM KH<sub>2</sub>PO<sub>4</sub> [pH7.4]) using fine forceps under a dissection microscope (S8APO, Leica; MZ FZ III, Leica). Pictures of the dissected tissues were taken by a digital camera (EC3, Leica) and the width of the CR and M4B were measured using ImageJ software (Schneider *et al.* 2012). To investigate the infection process, freshly dissected midguts were stained with 4',6-diamidino-2-phenylindole (DAPI) and observed under an epifluorescence microscope (DMI4000B, Leica). For analysis of phalloidin-stained tissues, the dissected midguts were fixed with 4% paraformaldehyde for 10 min at room temperature, washed twice in PBS, incubated in PBS containing 0.1% Triton X-100 for 5 min, stained with 0.5 μM of SYTOX Green and 5 units/ml of Alexa Fluor555 phalloidin (ThermoFisher) in PBS for 20 min, washed twice in PBS, and mounted on silane-coated glass slides and observed with a confocal laser scanning microscope (TCS SP8, Leica).

##### **Oral inoculation of colonization-deficient mutants and non-symbiotic bacteria**

Immediately after 1<sup>st</sup> instar nymphs molted to the 2<sup>nd</sup> instar, DWA was removed from the rearing containers so that the nymphs were kept without drinking water overnight and

became thirsty. Then DWA containing  $10^4$  cells/ $\mu\text{l}$  of each GFP-labelled strain was supplied to the rearing containers for 24 h. After 24 h, the symbiont-containing DWA was replaced by symbiont-free DWA, and the nymphs were further reared in the absence of bacteria during the instar. After the 2<sup>nd</sup> instar nymphs molted to 3<sup>rd</sup> instar, DWA containing  $10^4$  cells/ $\mu\text{l}$  of the RFP-labelled KT39 was supplied to the rearing containers for 24 h. These nymphs were further reared for two days with symbiont-free DWA, and then dissected to check their infection status of the GFP and RFP strains.

### **Bottleneck estimation**

To estimate how many symbiont cells can infect the symbiotic region before the midgut closure, co-inoculation of the GFP-labelled strain RPE225 ( $R_f^+$ ,  $K_m^+$ ) and the non-labelled wild type strain RPE75 ( $R_f^+$ ) was performed. The non-labelled symbiont and GFP-labelled symbiont were mixed in different ratios (GFP-labelled symbiont:non-labelled symbiont = 1:10, 1:10<sup>2</sup>, 1:10<sup>3</sup>, 1:1.65x10<sup>3</sup>, 1:5.0x10<sup>3</sup>, 1:10<sup>4</sup>, 1:1.5x10<sup>4</sup>, 1:4.6x10<sup>4</sup> or 1:2.2x10<sup>5</sup>). Symbiont cells were diluted in DWA to a cell density of 10<sup>5</sup> CFU/ $\mu\text{l}$ , and 2<sup>nd</sup> instar nymphs were fed with 1  $\mu\text{l}$  of the solution as above. Six to sixteen insects were inoculated per dilution. Three days after inoculation, the symbiotic organ (M4+M4B) was dissected and its content was plated on a YG plate containing kanamycin 30  $\mu\text{g}/\text{ml}$  to check whether GFP-labelled symbionts entered the symbiotic organ. Insects were counted as positive for infection with the GFP-labelled symbiont if at least one colony of the GFP-labelled symbiont was detected.

Schneider CA, Rasband WS, Eliceiri KW. NIH Image to ImageJ: 25 years of image analysis. *Nat Methods*. 2012; 9: 671-675.

**Table S1.** Bacterial strains used in this study.

Bacterial species/strain	Description	Fruorecent protein	Antibiotic resistance	Reference <sup>d</sup>
<b>Symbiont (<i>Burkholderia insecticola</i>)</b>				
<b>Wild type</b>				
RPE75	Rifampicin-resistant derivative of the type strain RPE64	none	Rif <sup>R</sup>	Kikuchi et al., AEM 2011 (1)
RPE225	GFP-labelled symbiont	GFP <sup>b</sup>	Km <sup>R</sup> , Cm <sup>R</sup>	Kikuchi&Fukatsu Mol Ecol 2014 (2)
KT39	RFP-labelled symbiont	RFP <sup>b</sup>	Km <sup>R</sup>	Itoh et al., PNAS, 2019 (3)
KT33 <sup>a</sup>	GFP-labelled, Cm-susceptible symbiont	GFP <sup>b</sup>	Km <sup>R</sup>	This study
RPE744 <sup>a</sup>	RFP-labelled, Cm-resistant symbiont	RFP <sup>c</sup>	Cm <sup>R</sup>	This study
<b>Colonization-deficient mutants</b>				
<i>flhC</i> ::Tn5	Flagella mutant; Reaches M3 but is blocked by CR	GFP <sup>b</sup>	Km <sup>R</sup> , Cm <sup>R</sup>	Ohbayashi et al. PNAS 2015 (4)
<i>purL</i> ::Tn5	Purine biosynthesis mutant; Poor crypt colonization	GFP <sup>b</sup>	Km <sup>R</sup> , Cm <sup>R</sup>	Kim et al., ISME J 2014 (5)
<i>Awaaf</i>	LPS biosynthesis mutant; Poor crypt colonization	GFP <sup>b</sup>	Km <sup>R</sup> , Cm <sup>R</sup>	Kim et al. JBC 2017 (6)
<i>AphaB</i>	PHA biosynthesis mutant; Poor crypt colonization	GFP <sup>b</sup>	Km <sup>R</sup> , Cm <sup>R</sup>	Kim et al. PNAS 2013 (7)
<b>Non-symbiotic bacteria</b>				
<i>Burkholderia fungorum</i> JCM21562	Colonizes crypts partially; Beneficial to the bean bug	GFP <sup>b</sup>	Km <sup>R</sup> , Cm <sup>R</sup>	Itoh et al., PNAS, 2019 (3)
<i>Pandoraea norimbergensis</i> JCM10565	Colonizes crypts partially; Beneficial to the bean bug	GFP <sup>b</sup>	Km <sup>R</sup> , Cm <sup>R</sup>	Itoh et al., PNAS, 2019 (3)
<i>Escherichia coli</i> WM3064	Reaches M3 but is blocked by CR	GFP <sup>b</sup>	Km <sup>R</sup>	This study
<i>Cupriavidus taiwanensis</i> DSM17343	Reaches M3 but is blocked by CR	GFP <sup>b</sup>	Km <sup>R</sup> , Cm <sup>R</sup>	Itoh et al., PNAS, 2019 (3)

<sup>a</sup>These strains were used in the experimental removal of crypt-colonizing symbionts by antibiotic treatment (Fig. 5).

<sup>b</sup>GFP/RFP was labelled by the Tn7 minitransposon system.

<sup>c</sup>RFP was labelled with the RFP-encoding stable plasmid pIN29.

<sup>d</sup>references: (1) Kikuchi Y, Meng XY, Fukatsu T. Gut symbiotic bacteria of the genus *Burkholderia* in the broad-headed bugs *Riptortus clavatus* and *Leptocoris chinensis* (Heteroptera: Alydidae). *Appl Environ Microbiol* 2005; **71**: 4035-4043; (2) Kikuchi Y, Fukatsu T. Live imaging of symbiosis: spatiotemporal infection dynamics of a GFP-labelled *Burkholderia* symbiont in the bean bug *Riptortus pedestris*. *Mol Ecol* 2014; **23**: 1445-1456; (3) Itoh H, Jang S, Takeshita K, Ohbayashi T, Ohnishi N, Meng XY *et al.* Host-symbiont specificity determined by microbe-microbe competition in an insect gut. *Proc Natl Acad Sci USA* 2019; **116**: 22673-22682; (4) Ohbayashi T, Takeshita K, Kitagawa W, Nikoh N, Koga R, Meng XY *et al.* Insect's intestinal organ for symbiont sorting. *Proc Natl Acad Sci USA* 2015; **112**: E5179-E5188; (5) Kim JK, Jang HA, Won YJ, Kikuchi Y, Heum Han S, Kim CH *et al.* Purine biosynthesis-deficient *Burkholderia* mutants are incapable of symbiotic accommodation in the stinkbug. *ISME J* 2014; **8**: 552-63; (6) Kim JK, Jang HA, Kim MS, Cho JH, Lee JB, Lorenzo FD *et al.* The lipopolysaccharide core oligosaccharide of *Burkholderia* plays a critical role in maintaining a proper gut symbiosis with the bean bug *Riptortus pedestris*. *J Biol Chem* 2017; **292**: 19226-19237; (7) Kim JK, Won YJ, Nikoh N, Nakayama H, Han SH, Kikuchi Y *et al.* Polyester synthesis genes associated with stress resistance are involved in an insect-bacterium symbiosis. *Proc Natl Acad Sci USA*. 2013; **110**: E2381-9.

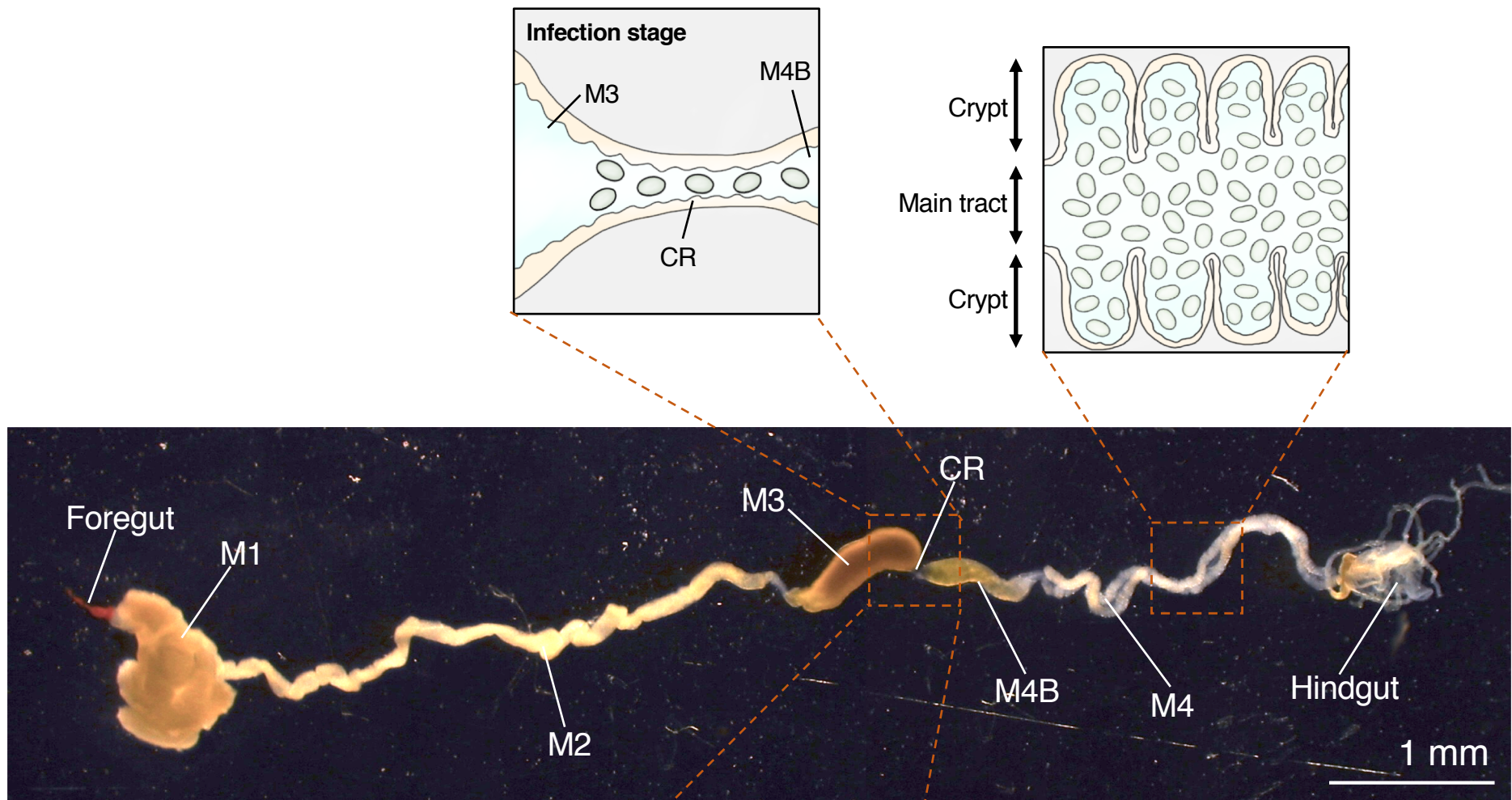


**Fig. S1. Whole gut of the bean bug *R. pedestris*.** The foregut, midgut (M1-M4), and hindgut are shown. The *Burkholderia* symbiont penetrates from M3 to M4B through the constricted region during infection. After colonization, the constricted region is closed and completely sealed (see Fig. 1, Fig. 2d, and Fig. S2). Abbreviations: M1, midgut 1<sup>st</sup> section; M2, midgut 2<sup>nd</sup> section; M3, midgut 3<sup>rd</sup> section; M4, midgut 4<sup>th</sup> section (crypt-bearing symbiotic region); CR, constricted region; M4B, M4 bulb.

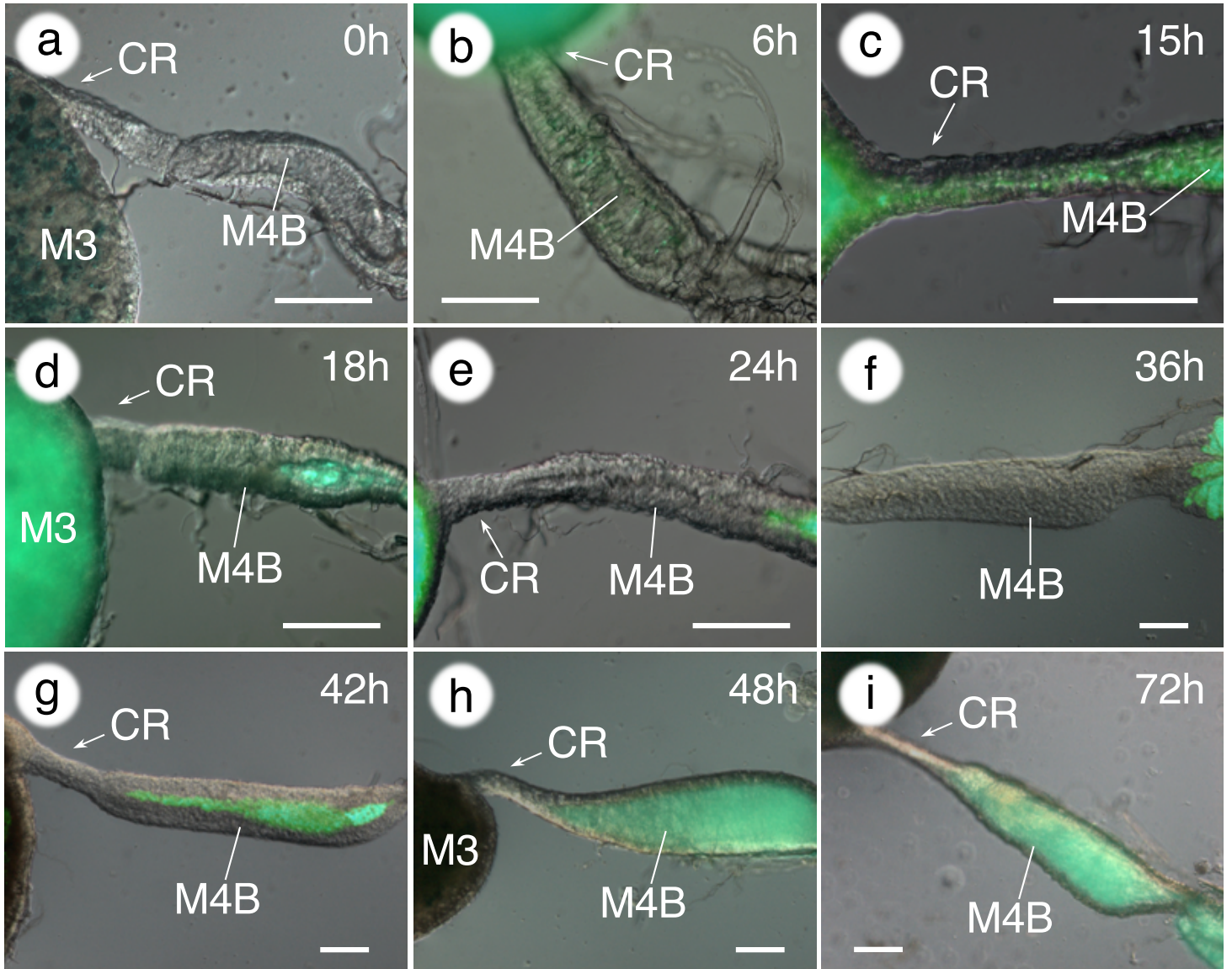


**Fig. S2. Morphological alteration of the constricted region and M4B during symbiont colonization in 2<sup>nd</sup> instar nymphs of *R. pedestris*.** (a-i) A GFP-labelled *Burkholderia* symbiont was orally administered, and the infection dynamics and morphogenesis of the M4B region were observed. Merged fluorescence and DIC images are shown. M4B is closed during symbiont infection (c-f) and reopened by backflow of symbiont cells during the colonization (g-i). Abbreviations: M3, midgut 3<sup>rd</sup> section; M4, midgut 4<sup>th</sup> section; CR, constricted region; M4B, M4 bulb. Bars: 0.1 mm.

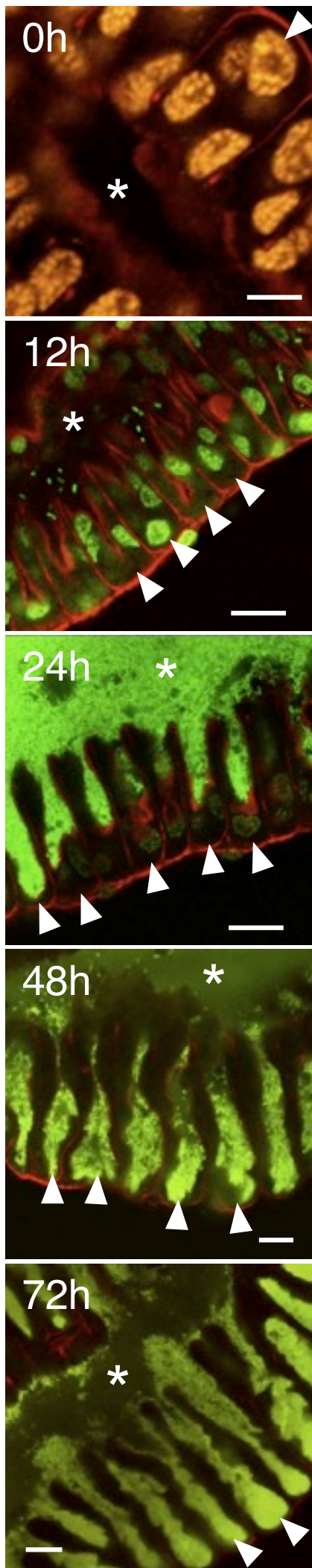


**Fig. S3. Infection dynamics of the GFP-labeled *Burkholderia* symbiont in M4 crypts of a 2<sup>nd</sup> instar nymph.** Symbiotic *Burkholderia* are visualized by GFP-labelling. Host cell nuclei are stained by SYTOX green, which are visualized as large yellow/green particles and are not clearly visible after 24 hours because of the high intensity of the GFP signals derived from the infecting bacteria. The actin cytoskeleton is stained by phalloidin (red) to visualize epithelial cells of crypts. Arrowheads indicate crypts. Asterisks indicate the main tract of the M4. Before inoculation (0h), crypts are not-well developed and their lumen is collapsed. At 12h after inoculation in the 2<sup>nd</sup> instar, symbionts start the colonization of the crypt lumen. Symbionts then proliferate inside the crypts and entirely fill their lumen after 48h post inoculation. Bars: 20  $\mu$ m.

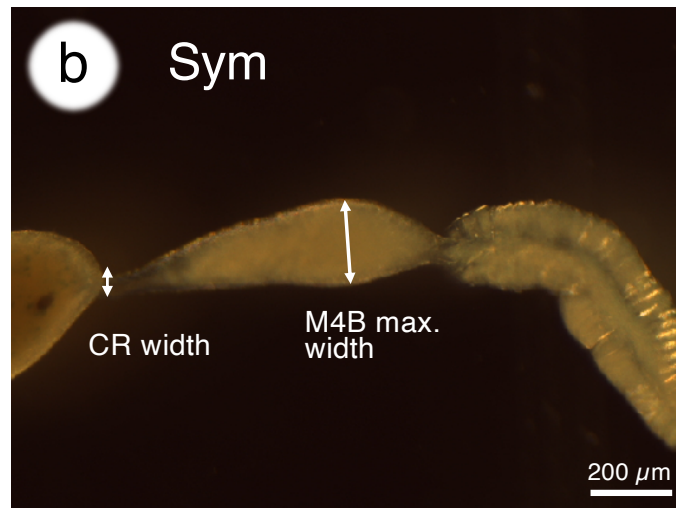
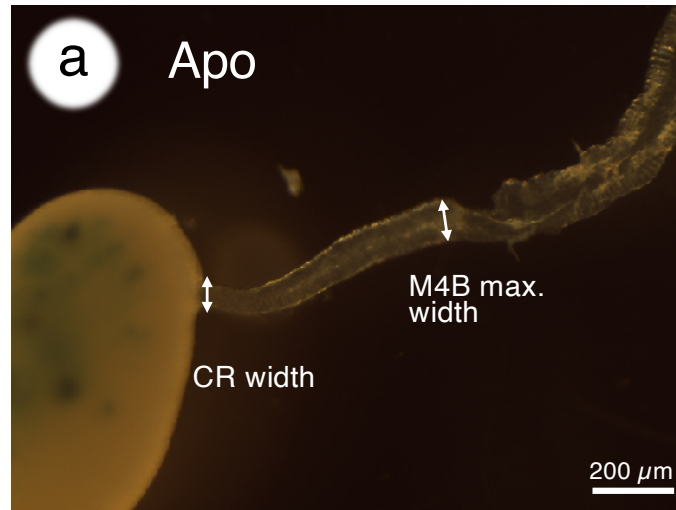


**Fig. S4. Measured parts of the constricted region and M4B.** The figure indicates the measurements performed for Fig. 1s and t. In M4B, the maximum width was measured.

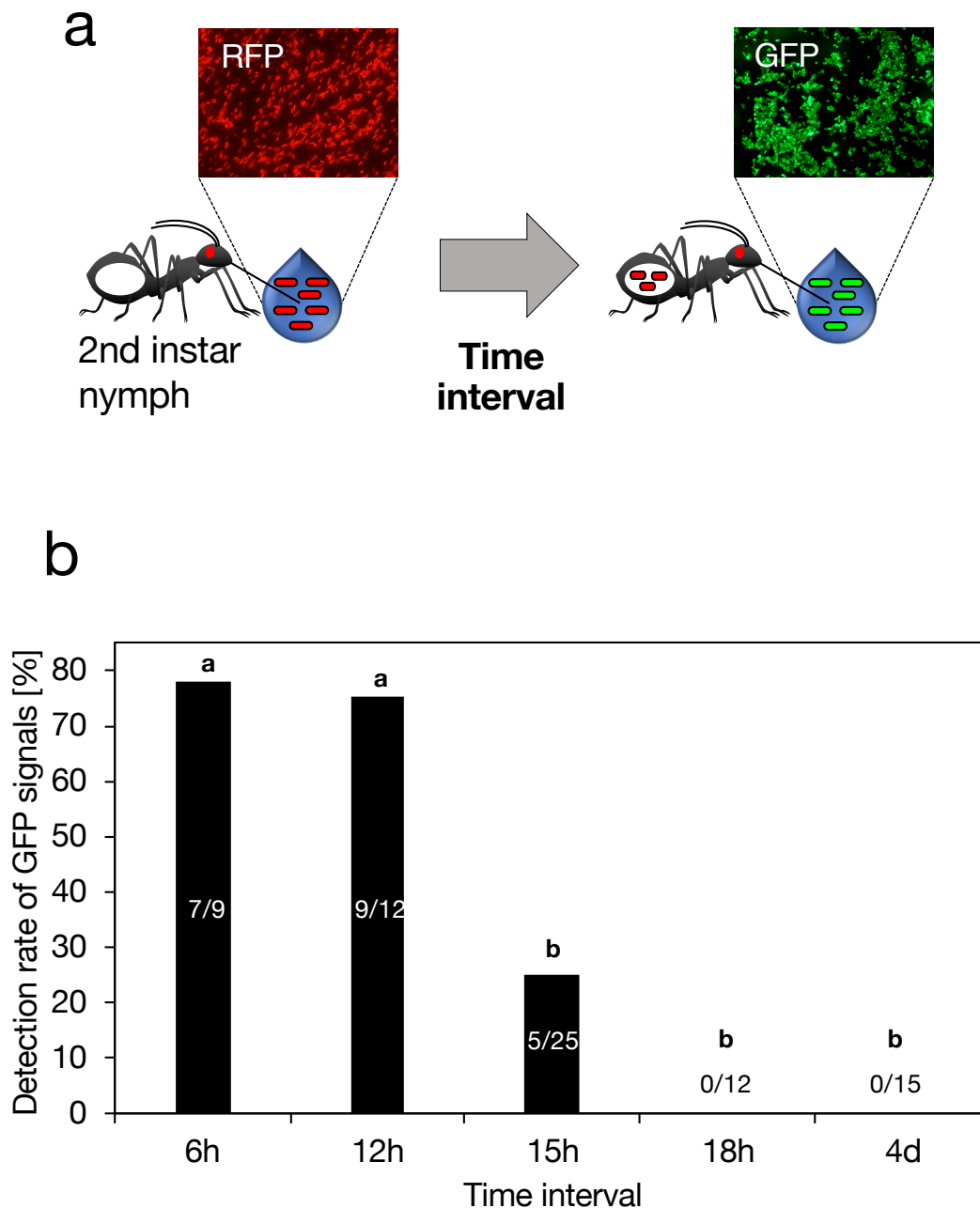


**Fig. S5. Experimental determination of the midgut closure timing.** (a) Experimental set-up of re-inoculation of the *Burkholderia* symbiont. An RFP-labelled symbiont was orally administered at the 2<sup>nd</sup> instar stage. After an interval of 6h, 12h, 15h, 18h or 3 days, a GFP-labelled symbiont was fed to the insects. In the 3-day-interval group, insects molted to 3<sup>rd</sup> instar during the interval, and the molted insects were fed with the GFP-labelled symbiont. Three days after infection of the GFP-labelled symbiont, insects were dissected and fluorescence signals were observed by fluorescence microscopy. (b) Detection rate of GFP signals at the symbiotic region (M4B+M4) after the re-inoculation test. RFP signals were detected in all tested individuals. The ratio of GFP-positive insects to all tested insects is depicted in the histograms. Different letters above the bars indicate a significant difference between groups by the Fisher's exact test after the Bonferroni correction ( $P < 0.05$ ). Raw data (pictures) are shown in Supplementary Fig. S5.

## 6h interval

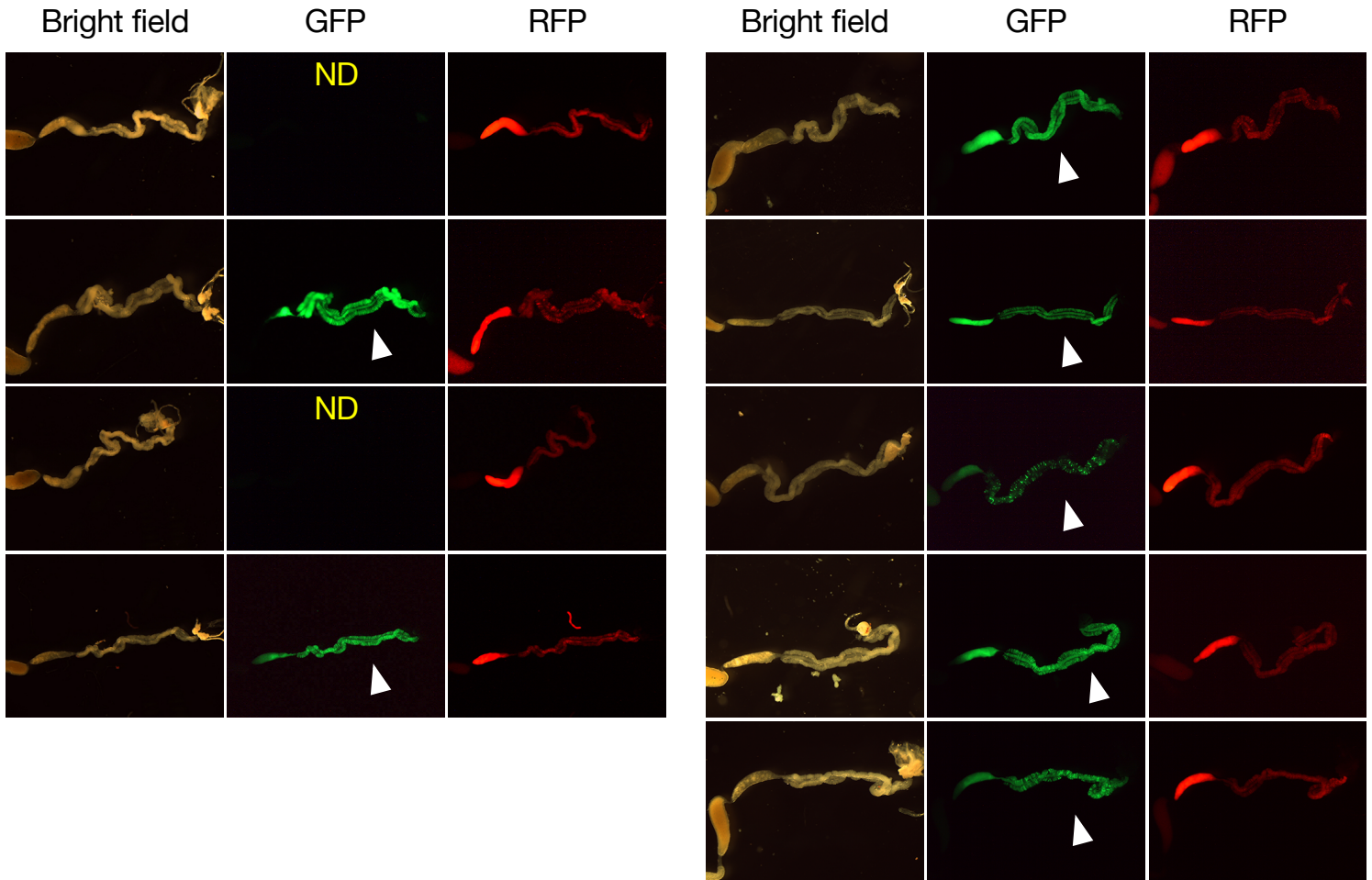


**Fig. S6. Picture data of the re-inoculation test summarized in Fig. S4b.** The re-inoculation of a GFP-labelled symbiont strain was done at 6h, 12h, 15h, 18h and 3 days intervals after the first infection with an RFP strain. Arrowheads indicate infection of the GFP strain. ND: GFP signal not detected.

## 12h interval

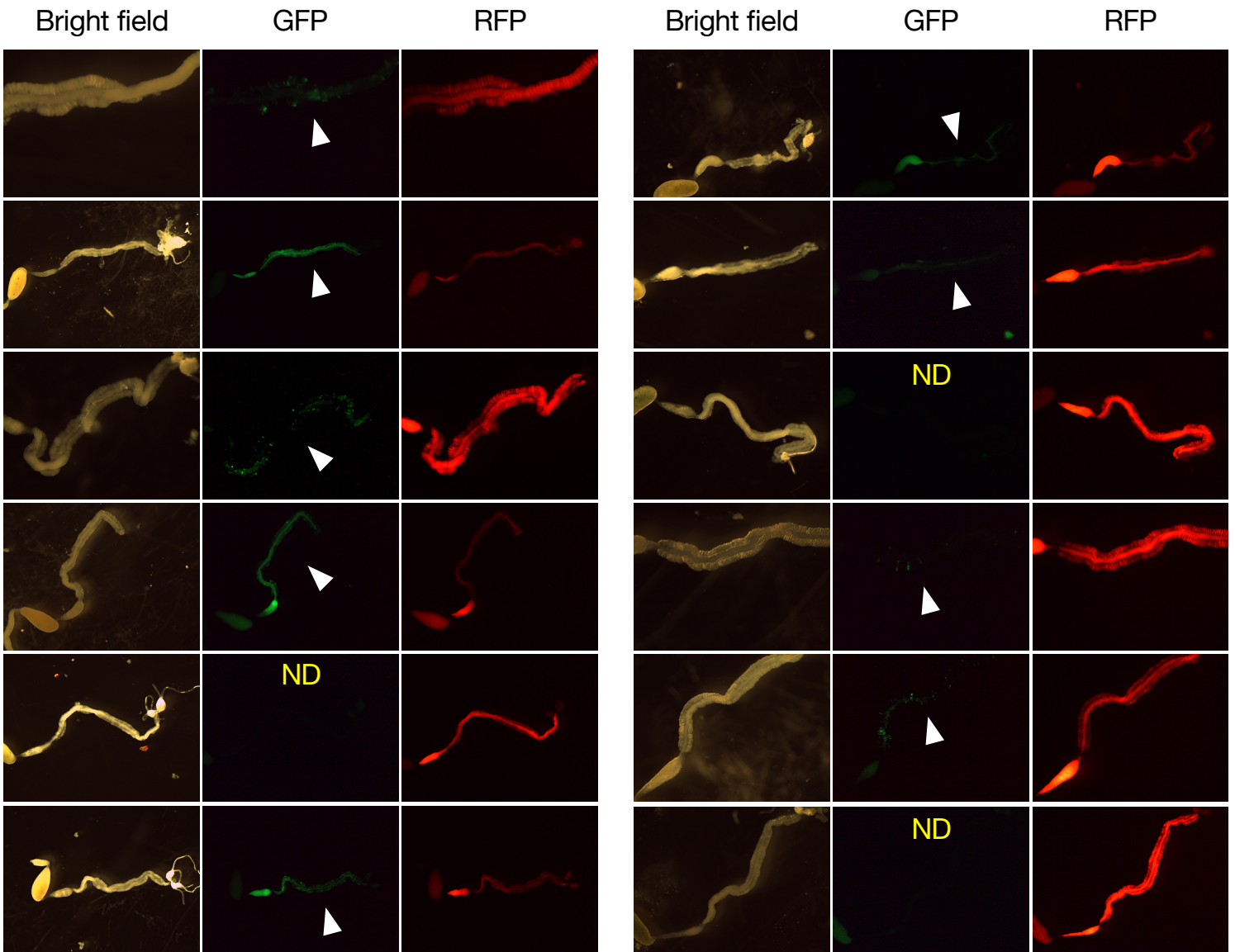
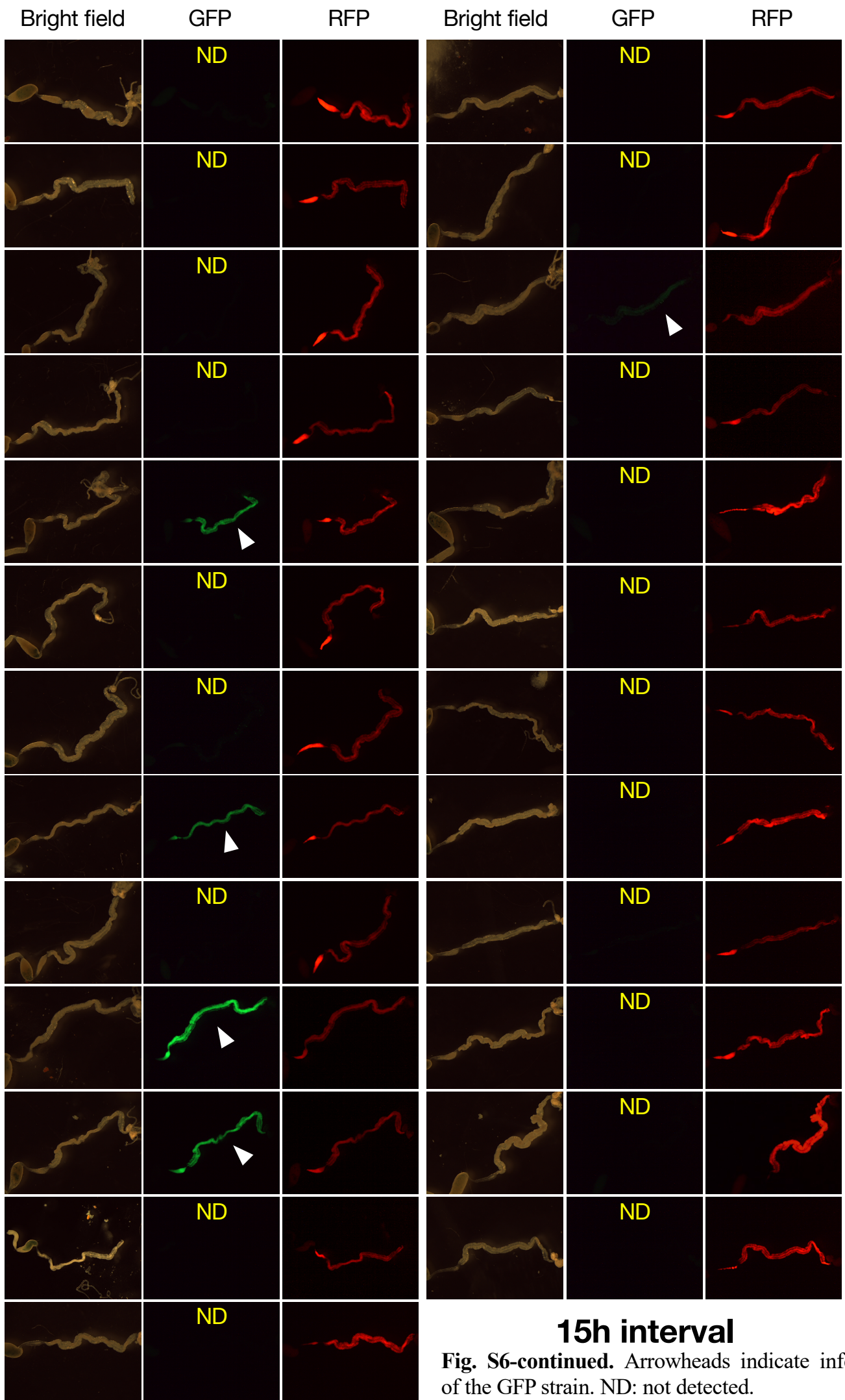


**Fig. S6-continued.** Arrowheads indicate infection of the GFP strain. ND: not detected.



**15h interval**

**Fig. S6-continued.** Arrowheads indicate infection of the GFP strain. ND: not detected.

## 18h interval

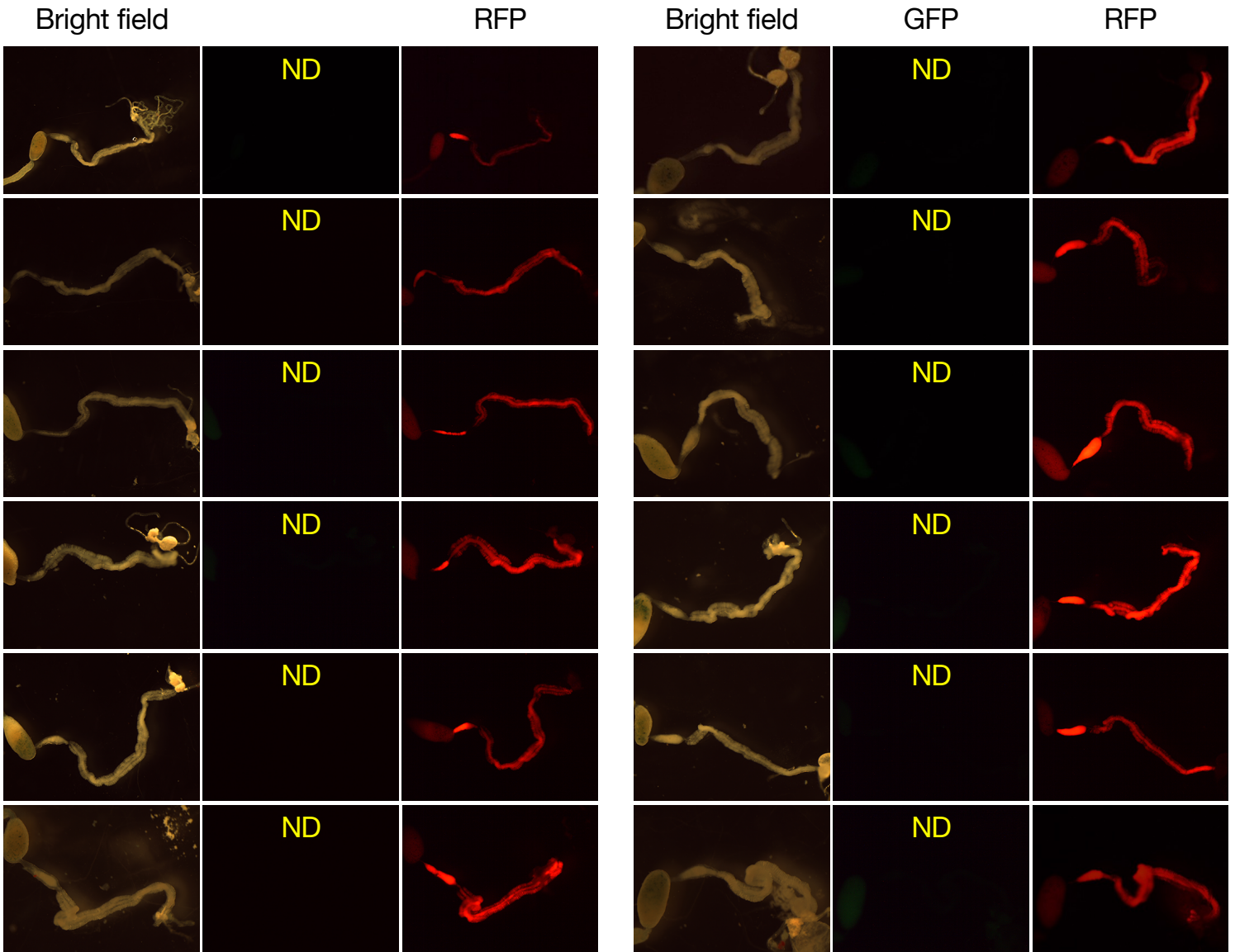


**Fig. S6-continued.** Arrowheads indicate infection of the GFP strain. ND: not detected.

### 3 days interval

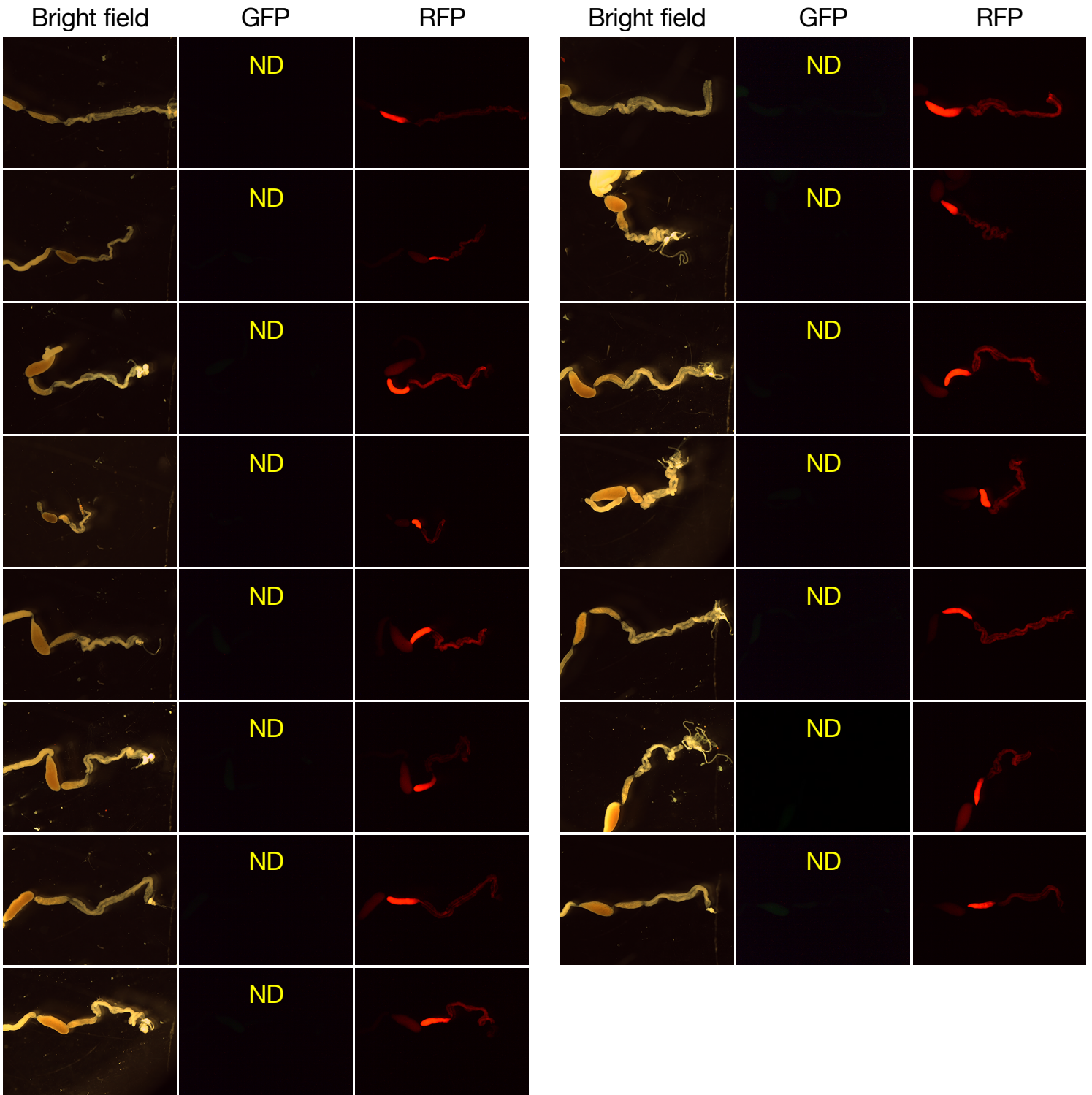


**Fig. S6-continued.** Arrowheads indicate infection of the GFP strain. ND: not detected.

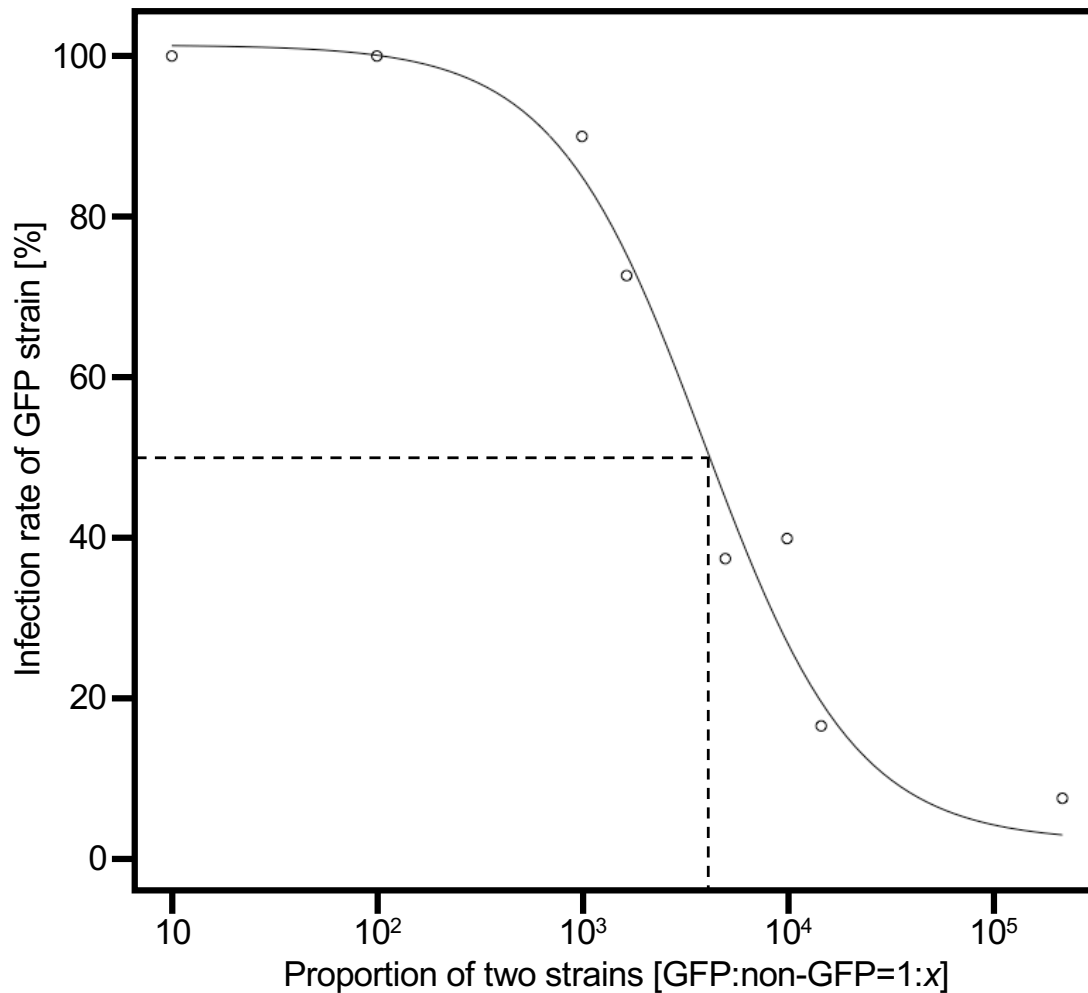


**Fig. S7. The constricted region and midgut closure create a bottleneck on the symbiont population.** In the oral administration experiments, second-instar nymphs were fed with GFP-labelled and non-labelled symbiont strains, mixed in different ratios (1:10; 1:10<sup>2</sup>; 1:10<sup>3</sup>; 1:1.65x10<sup>3</sup>; 1:5.0x10<sup>3</sup>; 1:10<sup>4</sup>; 1:1.5x10<sup>4</sup>; 1: 4.6x10<sup>4</sup> and 1:2.2x10<sup>5</sup>), and the percentage of host individuals colonized by the GFP-labelled symbiont was subsequently determined by plating on selective medium. The dilution ratio at which 50% of the bean bugs carry the GFP-labelled symbiont, indicated by the dotted lines, was determined by using the *drc* package in R software; the equation probit is  $(y) = 2.2913 + 99.08 / (1 + \exp(1.18 * (x - 3950)))$ .